Havacılıkta Kullanılan 2000 Ve 6000 Serisi Alüminyum Alaşımlarının Mekanik Ve Korozyon Davranışlarında Kriojenik İşlemin Etkisi

Kamil Burak GÖÇMEN

YÜKSEK LİSANS TEZİ

Havacılık Bilimi ve Teknolojileri Anabilim Dalı

Kasım 2021

The Effect Of Cryogenic Treatment On The Mechanical And Corrosion Behaviors Of Aluminum Alloys 2000 And 6000 Series Used In Aviation

Kamil Burak GÖÇMEN

MASTER OF SCIENCE THESIS

Department of Aviation Science and Technologies

November 2021

The Effect Of Cryogenic Treatment On The Mechanical And Corrosion Behaviors Of Aluminum Alloys 2000 And 6000 Series Used In Aviation

Kamil Burak GÖÇMEN

A thesis submitted to Eskişehir Osmangazi University
Graduate School of Natural and Applied Sciences in partial
fulfillment of the requirements for the degree of Master of Science
in Department of Aviation Science and Technologies

Supervisor: Doç. Dr. Mustafa Özgür ÖTEYAKA

November 2021

ETHICAL STATEMENT

I hereby declare that this thesis study entitled “Havacılıkta Kullanılan 2000 Ve 6000 Serisi Alüminyum Alaşımlarının Mekanik Ve Korozyon Davranışlarında Kriojenik Işlemin Etkisi” has been prepared in accordance with the thesis writing rules of Eskişehir Osmangazi University Graduate School of Natural and Applied Sciences under academic consultancy of my supervisor Assoc. Prof. Dr. Mustafa Özgür ÖTEYAKA. I hereby declare that the work presented in this thesis is original. I also declare that, I have respected scientific ethical principle and rules in all stages of my thesis study, all information and data presented in this thesis have been obtained within the scope of scientific and academic ethical principles and rules, all materials used in this thesis which are not original to this work have been fully cited and referenced, and all knowledge, documents and results have been presented in accordance with scientific ethical principles and rules. 04/11/2021

Kamil Burak GÖÇMEN

Signature

ÖZET

Alüminyum alaşımları hafif, korozyon direnci ve mekanik özelliklerinin iyi olmasından dolayı farklı sektörlerde kullanılmaktadır. Havacılık sektöründe mukavemet istenen yerlerde 2000 serisi ve yapısal uygulamalarda 6000 serisi tercih edilmektedir. 2000 serisi içinde başlıca Cu elementi, 6000 serisinde ise Si ve Mg elementleri mevcuttur. Bu alaşımlar ısıl işleme yatkın alaşımlardır; 2000 serisine uygulanan ısıl işlem sonunda mukavemette artış kazanılırken korozyon özelliklerinde düşüş, 6000 serisinde ise korozyon özelliklerinde ve şekil alma kabiliyetinde artış sağlar. Son yıllarda, alüminyum alaşımlarının mekanik ve korozyon özelliklerini iyileştirmek için -196 ^{o}C'de farklı sürelerde kriyojenik ısıl işlemi uygulanmaktadır. Bu işlem sonunda mikroyapıda tanelerin incelmesi ve ikincil fazların (intermetallik fazların) homojen dağıldığı gözlemlenmiştir. Bu değişim mekanik ve korozyon özelliklerinde iyileşme sağlamıştır. Yapılan çalışmada, havacılıkta kullanılan 2024-T0, 2024-T3, 6061-T0 ve 6061-T6 alüminyum alaşımlarına 8 h, 16 h ve 24 h sürelerde kriyojenik ısıl işlemi uygulanarak mekanik ve korozyon özellikleri incelenmiştir. Elde edilen sonuçlara göre, kriyojenik ısıl işlem görmüş 2024-T3 ve 6061-T6 numunelerde % 14 sertlik artışı gözlemlenmiştir. Sertlik değeri 2024-T3 için 24h kriyojenik ısıl işlem sonunda 155 HV değerine ulaştı. Ayrıca, 6061-T6 alaşım için 24 h kriyojenik işlem sonunda 129 HV değerine ulaşmıştır. Çekme deneyi sonucunda 2024-T3-8h numune çekme mukavemeti ve % uzama değerleri diğer 2024-T3 numunelere göre yüksek bulunmuştur. Diğer taraftan, 6061-T0 için akma mukavemetinde 6061-T0-16h ve 6061-T0-24h numunelerde % 2 artış sağlanmıştır. Ayrıca 6061-T6 için en yüksek akma mukavemeti değeri 16 h kriyojenik ısıl işlem sonrası gözlemlenmiştir. Korozyon deneyleri sonuçları incelendiğinde, passivasyon bölgesi tüm numunelerde gözlemlenmiştir. Serbest korozyon potansiyeli ölçümü deneyinde 6061-T6-8h diğer 6061-T6 numunelere göre korozyon potansiyeli daha anodik bulunmuştur. Diğer taraftan EIS sonuçları incelendiğinde 6061-T6 ısıl işlem görmüş numunelerin koroyzon direnci daha yüksek tespit edilmiştir.

Anahtar Kelimeler: Alüminyum alaşımları, 2024 alaşımı, 6061 alaşımı, ısıl işlem, mekanik özellikler, korozyon.

SUMMARY

Aluminum alloys are used in different sectors for their lightweight, corrosion resistant and have good mechanical properties. In the aviation industry and in structural applications where strength is required 2000 series and 6000 series is preferred. In the 2000 series, Cu and in the 6000 series Si and Mg are major elements available. These alloys are heat treatable alloys; At the end of the heat treatment applied to the 2000 series, an increase in strength is gained in adverse corrosion decrease while in the 6000 series an increase in corrosion properties and shaping ability. In recent years, to improve the mechanical and corrosion properties of the aluminum alloys cryogenic heat treatment is applied in different times at -196 oC. At the end of this process, it was observed in the microstructure a secondary phases (intermetallic phases) were homogeneously dispersed and the grains is thinned. This change in microstructure improved the mechanical and the corrosion properties. In this study, the mechanical and corrosion properties of 2024-T0, 2024-T3, 6061-T0 and 6061-T6 aluminum alloys used in aviation were investigated by applying cryogenic heat treatment for 8 h, 16 h and 24 h. According to the results obtained, the hardness increased about 14 % after cryogenic heat treatment fort he alloy 2024-T3 and 6061-T6 samples. The hardness value reached 155 HV after 24h of cryogenic heat treatment for 2024-T3. In addition, it reached 129 HV for 6061-T6 alloy after 24 h cryogenic treatment. On the other hand, , an 2% increase was achieved in yield strength for 6061-T0-16h and 6061-T0-24h samples compared to 6061-T0. In addition, the highest yield strength value for 6061-T6 was observed after 16 h cryogenic heat treatment. When the corrosion test results were examined, the passivation zone was observed in all samples. In the free corrosion potential measurement test, the corrosion potential of 6061-T6-8h was found to be more anodic than the other 6061-T6 samples. Moreover, the corrosion resistance of the 6061-T6 heat-treated samples was found to be higher regarding the EIS findings.

Keywords: Aluminum alloys, 2024 alloy, 6061 alloy, heat treatment, mechanic properties, corrosion.

LIST OF CONTENTS

. **Page**

LIST OF FIGURES

Figure **Page**

LIST OF FIGURES (continued)

Figure **Page**

LIST OF TABLES

Table **Page**

1. INTRODUCTION

Aluminum (2.7 g/cm^3) is used in the automotive and aerospace industries because it is 1/3 lighter than steels and because it reaches the strength values of common steels with heat treatments (Committee 1990; Jovičević-Klug and Podgornik 2020; Ma et al., 2004; Macário et al., 2019). The tensile strength of pure Al metal is 90 MPa. The addition of the alloying elements and the applied heat treatment to the pure metal, this value goes up to 455 MPa (2000 series). When the corrosion properties are examined, it provides protection by forming a metal oxide film in the air environment (Fahimpour et al., 2012; Mascagni et al., 2014). Although the oxide film is resistant in humid, industrial, and acidic environments, it is not resistant to alkaline environments (Kaseem et al., 2015; Macário et al., 2019; Reboul and Baroux 2011). Aluminum alloys are easy to cast and produce as sheet metal. Forged alloys with a 4-digit coding system are classified; the most commonly used alloy series in aviation are the 2xxx, 5xxx, 6xxx, and 7xxx series. Aluminum alloys have an important place in the aviation industry. The reason is that they are light and with applied heat treatments, their strength is close to medium carbon steel. The most preferred aluminum alloy series are the 2xxx, ,6xxx and 7xxx series. On the other hand, aluminum parts used in aviation should be replaced after a certain period.

Cryogenic heat treatment is a heat treatment applied to materials in a liquid nitrogen environment at -196 ^{o}C. This change in physical properties is a result of changes in microstructure at the end of the process. While this process gives good results in steel, however ,the effect on light metals is under investigation. Overwork on aluminum alloys, it is observed that the microstructure becomes more homogenous and the secondary phases are resolved in the matrix. Specified after cryogenic heat treatment. In addition, it has been determined that there is an increase in strength and hardness for some alloys.

The effect of cryogenic heat treatment on light metals in recent times is being investigated. At the end of this process, it has been observed an increase in the mechanical properties and corrosion resistance. In this context, this study investigates the cryogenic heat treatment effect on the mechanical and corrosion behavior of 2024-T0, 2024-T3, 6061-T0, and 6061-T6 aluminum alloys.

2. LITERATURE REVIEW

2.1 Aluminum alloys and aviation application

Aluminum alloys are widely used in different industries such as automotive, aviation (*Figure 2.1*), etc.(Cole and Sherman 1995; Committee 1990; Dursun and Soutis 2014; Jovičević-Klug and Podgornik 2020; Salguero et al., 2020; Zheng et al., 2018); because of lightweight (2.74 g/cm^3), good mechanical properties (*Figure 2.2*) and corrosion resistance compared to other materials. In the automotive industry the aluminum alloys were used in powertrain (casting), chassis (casting and wrought) and body (wrought) structure. For example, the Audi A8 has used 348 kg of aluminum alloys which reduced the car weight from 1348 kg to 1121 kg (Cole and Sherman 1995).

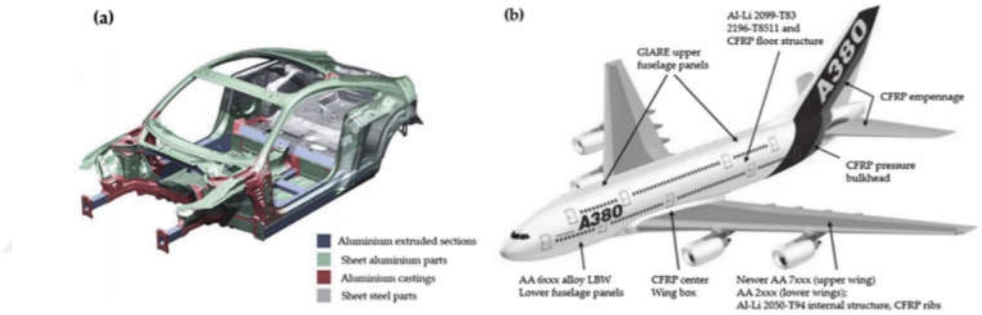

Figure 2.1.Aluminum use in automotive and aviation a) Audi TT coupé and b) A380 (Zheng et al., 2018).

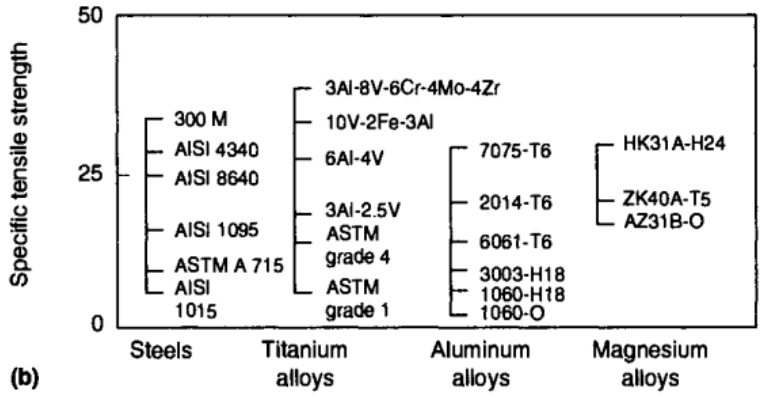

Figure 2.2.Comparisons of specific tensile strength of aluminum alloys versus different alloys (Committee 1990).

On the other hand, the aviation also followed in parallel the performance of automotive to reduce the weight of the airplane (*Figure 2.3*). The weight reduction involves fuel reduction, increasing the range and the payload. Moreover, optimization of materials can also reduce the maintenance time and repair cost (Dursun and Soutis 2014). It is especially used in 2xxx, 6xxx and 7xxx (Table 2.*1*) series aircraft fuselage and wings (Salguero et al., 2020). Various methods are used to increase the mechanical properties and corrosion resistance of these alloys. These are mainly heat treatment, addition of new alloying elements or their ratios modification and production methods.

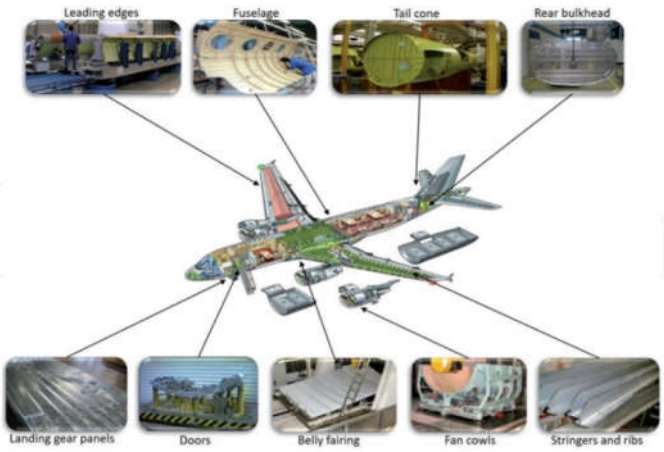

Figure 2.3. A319 aircraft structural parts (Salguero et al., 2020).

Table 2.1. Some aluminum alloys used in aeronautical; properties, composition and alloy designation (Salguero et al., 2020).

Identification	Aluminum Association	AA2024	AA7475	AA7050	AA7075
	UNS	A92024	A97475	A97050	A97075
	ISO	AlCu4Mg1	AlZn5.5MgCu(A)	AlZn6CuMgZr	AlZn5.5MgCu
Composition	Si	≤0.5	≤0.1	≤0.12	≤0.4
	Fe	≤0.5	≤0.12	≤0.15	≤0.5
	Cu	3.8–4.9	1.2–1.9	1.9–2.5	1.2–2.0
	Mn	0.3–0.9	≤0.06	≤0.1	≤0.3
	Mg	1.2–1.8	1.9–2.6	2.0–2.7	2.1–2.9
	Cr	≤0.1	0.18–0.25	≤0.04	0.18–0.28
	Zn	≤0.25	5.2–6.2	5.9–6.9	5.1–6.1
	Ti	≤0.15	≤0.05	≤0.06	≤0.2
	Al	Rem.	Rem.	Rem.	Rem.
Properties	Density (kg/m^3)	2.78	2.81	2.83	2.81
	Melting point (°C)	500–638	477–635	490–630	475–635
	Thermal conductivity (W/m°C)	121–151	163	157	130
	Thermal expansion (um/m°C)	23.2	23.2	24.1	23.6
	Young's Modulus (GPa)	73	72	72	72
	Percent elongation (%)	6–20	12	10	11
	Ultimate tensile strength-UTS (MPa)	440–495	531	495–550	525–570
	Heat treatment	T3, T4, T361, T6, T81,T861	T7651	T74	T6, T651, T73

Among them, the 2xxx series is the most preferred. The strength value after applied cold forming and heat treatment is equivalent to medium carbon steel. Airframe and wing It is used in parts of [9]. The 6xxx series, on the other hand, is preferred like the 2xxx series in aircraft fuselage and wing parts due to its easy welding ability and heat treatment (Fahimpour et al., 2012; Kaseem et al., 2015; Reboul and Baroux 2011).

Different alloy ratios, production methods and heat treatments are applied to aluminum alloys to improve strength and corrosion properties [12]. Recently, researches to improve these

properties with cryogenic heat treatment have gained momentum. This process was first applied to cutting steel tools in 1940 and an increase in mechanical properties was observed.

In the literature, cryogenic heat treatment has been applied to aluminum alloys at different times (Padmini et al., 2019a; Park et al., 2015). For example, 2024-T351 alloy was cryogenic heat treated for 2, 6, 8, 12 and 24 hours. At the end of this process, the defects in the microstructure and the precipitated secondary phases affect the distribution. they have observed. In addition, an increase in strength values and 24-hour cryogenic heat treatment The highest value after 480.6 MPa was obtained (*Figure 2.4*). In this study, the hardness and corrosion properties have not been investigated (Zhou et al., 2016).

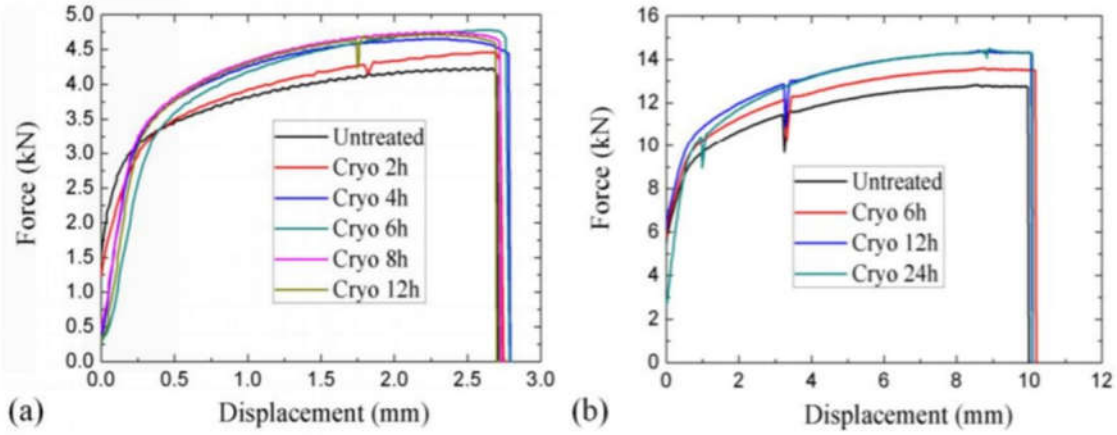

Figure 2.4. 2024-T351 aluminum alloy tensile curves; a) N1-0-N1-5 b) N2-0-N2-3(Zhou et al., 2016) .

The microstructure of the cryogenic treated sample 2024-T351 were presented at *Figure 2.5*. It was observed lower defects for the sample cryogenic treated for 6h (*Figure 2.5c*). Moreover, the precipitates were more uniform dispersed in the microstructure compared to untreated sample (Zhou et al., 2016).

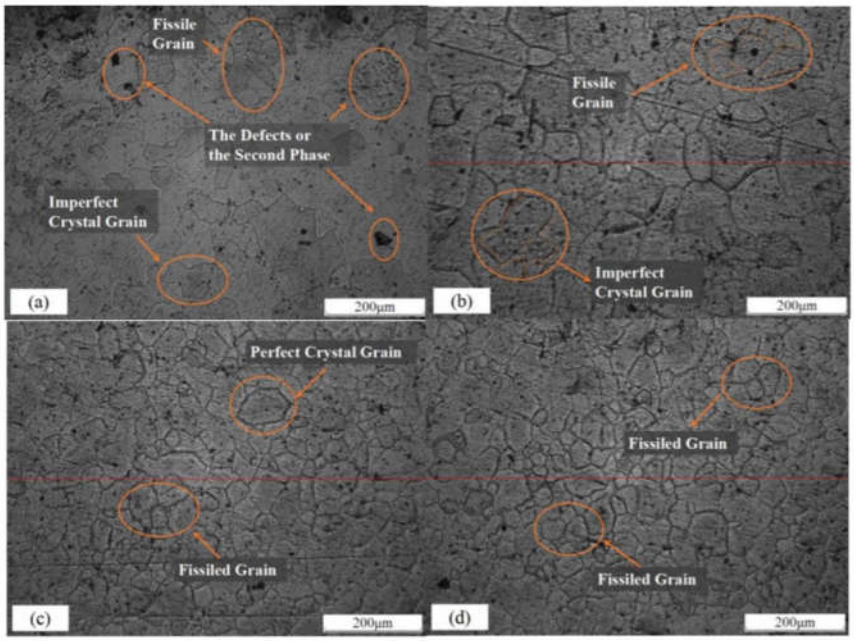

Figure 2.5. 2024-T351 aluminum alloy; microstructure images a) untreated, b) CT-2h, c) CT-6h and d) CT- 12h (Zhou et al., 2016).

A similar study was performed by Padmini et al. (Padmini et al., 2019a); 2, 9 and 64 hours of cryogenic treatment was applied to 2024, 7075 and 602 aluminum alloys and a 24% improvement was found for the wear amount of the 2024 alloy. Lulay et al. (Lulay et al., 2002) used 7075 alloy and applied cryogenic heat treatment at -196 ºC at two different retention times; 2h and 48h. Because of the analysis, the shrinkage compared to the original sample increased the strength of 1.5% and the impact of 11.5% after 48 h of cryogenic heat treatment.

In another study, cryogenic heat treatment was applied to the welded aerospace Al alloys for 48 h. In the analyzes of the parts, the stress corrosion cracking was improved (*Figure 2. 6*). Residual stress in the welded area from 23.9 ksi has fallen to to 12.2 ksi (Table 2.*2*) . On the other hand, a slight increase in strength and hardness was observed (Chen et al., 2001).

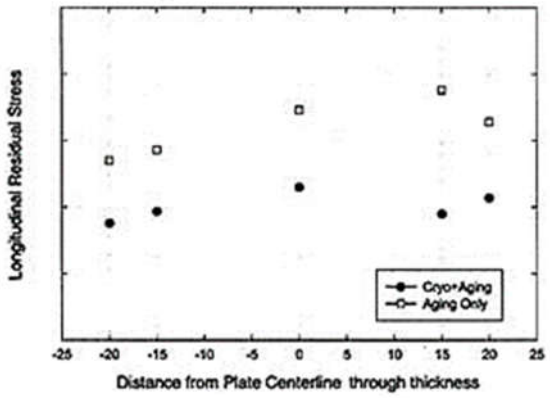

Figure 2. 6.Longitudinal residual stress profiles of aluminum alloy (Chen et al., 2001).

Table 2.2. Aluminum alloys welds stress corrosion (Chen et al., 2001).

Specimen Condition	Stress Level (%YS)	Failure Ratio	Highest Residual Stress in HAZ	Days to Failure
As-welded	50	1/3	23.9 ksi	65
	75	2/3		3, 6
Cryogenically treated	50	0/3	12.2 ksi	--
	75	2/3		22, 84

On the other hand, the effect of short-term instead of long-term cryogenic treatment on LC4 (Al-Zn-Mg-Cu) aluminum alloy was investigated by Zhang et al. (Zhang et al., 2013). Cryogenic heat treatment was applied at -196 °C for 40 minutes. After this process, mechanical properties and corrosion resistance in 3.5 wt% NaCl solution were measured. It was observed that the precipitates in the microstructure after the cryogenic treatment dissolved in the matrix and the secondary phases were located in the form of chains at the grain boundary. In addition, the samples treated with cryogenic heat treatment and cryogenic heat treatment followed by 24 h aging at 120 °C were subjected to compression test; the cryogenic treatment improved 25.69 % and 59.72 % compared to the original sample. In the same study, the corrosion potential of the original sample which was -834 mV increased up to -805 mV after cryogenic treatment and aging. They found that this improvement resulted in the reduction of secondary phases in the microstructure and, as a result, a decrease in galvanic interaction (*Figure 2.7and Figure 2.8*).

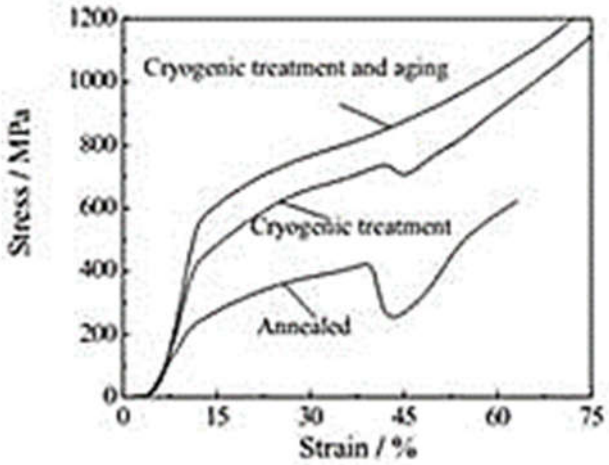

Figure 2.7. Untreated and treated LC4 (Al-Zn-Mg-Cu) alloy compression test results.

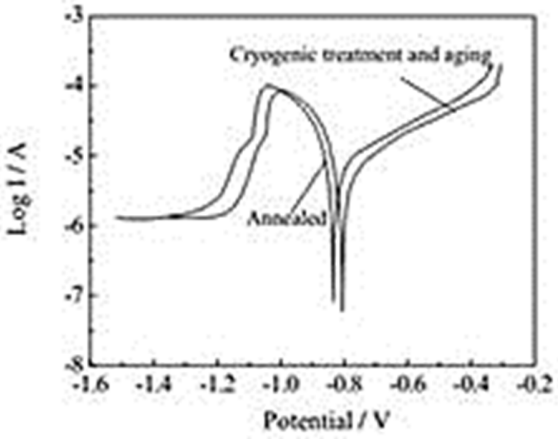

Figure 2.8. Potentiodynamic test of untreated and treated LC4 (Al-Zn-Mg-Cu).

A decrease in wear rate was observed after 12 hours of cryogenic heat treatment applied to 6101 aluminum alloy. The reason for this is related to that the GP regions (Guinier-Preston) dissolved in the matrix at the end of this heat treatment and therefore the wear performance is improved (Franco Steier et al., 2016).

Cryogenic heat treatment was applied to 6061 metal matrix composite materials. Varun Chandra et al. (Varun Chandra et al., 2018) applied cryogenic heat treatment by adding B4C+Gr to 6061 alloy at different level. At the end of this study, it was stated that there was an increase in strength and hardness in heat treated composites, and B4C+Gr (12 %) aluminum composite. In another study, an increase in mechanical properties was observed after cryogenic heat treatment applied to LC25 aluminum composite with SiC additives (Elango et al., 2014).

2.2 Corrosion of aluminum alloys

2.2.1 Corrosion behavior of 2000 aluminum alloy

The corrosion of 2024 aluminum alloys was due mainly of intermetallic phase formation due to addition of Cu and Mg (Siskou et al., 2018). Different studies were performed on the corrosion of 2024 aluminum alloys. Localised corrosion was observed on the surface of aluminum alloy such as pitting, intergranular and stress corrosion cracking (Pantelakis et al., 2016; Pantelakis et al., 2012; Valerie and Georges 1999) and galvanic corrosion (*Figure 2.9*) (Snihirova et al., 2019).

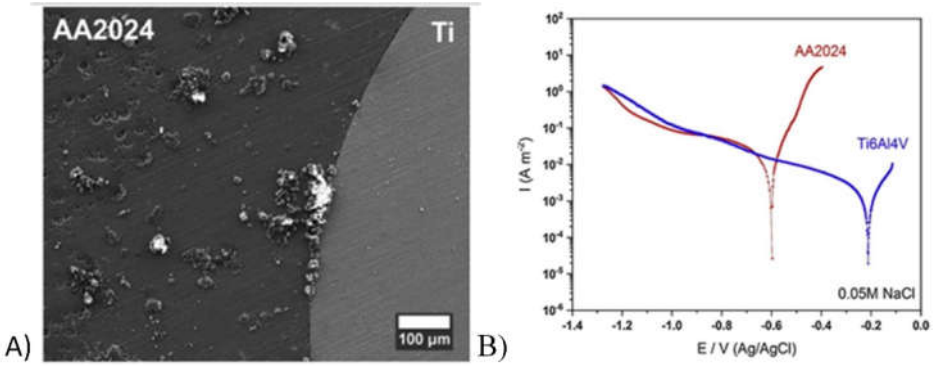

Figure 2.9. AA2024-Ti galvanic couple A) after 25 h of immersion and B) potentiodyanmic curves in 0.05 M NaCl (Snihirova et al., 2019).

For this reason, some coating was applied to reduce the corrosion rate. For example, Macario et al. applied diamond -like carbon (DLC) films on Al2024 -T3, Al5052 -H32, and Al6061 -T6 aluminum alloys (Macário et al., 2019). Different application was also applied on

the surface of aluminum alloy such as anodization of the surface to protect the aluminum alloys against corrosion (Dasquet et al., 2000; Shi et al., 2013; Xiangfeng et al., 2013), plasma coating (Mascagni et al., 2014).

2.2.2 Corrosion behavior of 6000 aluminum alloy

The corrosion performance of the 6063 alloy was studied by Prabhu and Rao (Deepa and Padmalatha 2017) in sodium hydroxide medium and phosphoric acid medium. The tafel polarisation of the alloy in H_3PO_4 was presented at *Figure 2.10*. It can be seen that decreasing the amount of H_3PO_4 make more anodic the corrosion potential. Moreover, the corrosion behavior of 6063 alloy was evaluated using EIS (*Figure 2.11*). The results show that the corrosion was principally charge transfer controlled in H_3PO_4.

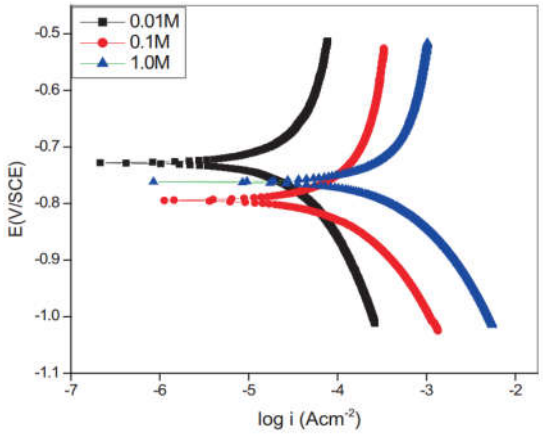

Figure 2.10. Anodic curve of 6063 alloy in different concentration of H_3PO_4 at 30 ^oC (Deepa and Padmalatha 2017) .

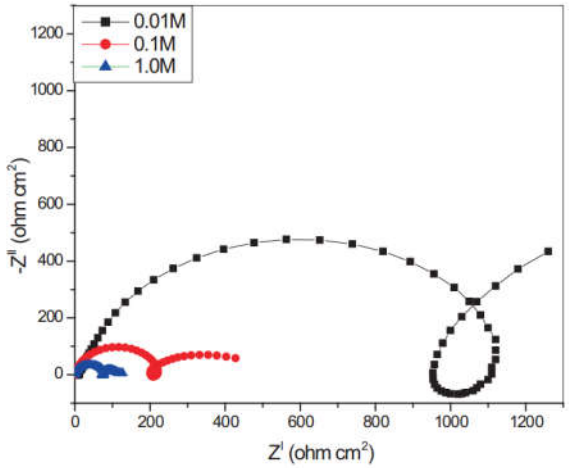

Figure 2.11. The Nyquist curves of 6063 alloy in different concentration of H_3PO_4 at 30 °C (Deepa and Padmalatha 2017).

Fahimpour et al. examined the corrosion performance of 6061 alloy joined by friction stir welding (Fahimpour et al., 2012). The corrosion resistance was found lower in the weld region. Moreover, the T6 treatment increased the corrosion potential of 6061 alloy. In another work, Huang et al. (Huang et al., 2008) investigated by EIS the corrosion performance of anodized 6061 alloy. The results showed that the porous film formed using hard anodizing on the surface of 6061 alloy exhibited better corrosion resistance.

2.3 Mechanical performance of aluminum alloys

2.3.1 Mechanical performance of 2000 aluminum alloys

The mechanical properties such as tensile strength, hardness, wear performance, etc. should be determined before to use in the industry. Bekheet et al. examined the wear and hardness of the composite 2024-SiC material (Bekheet et al., 2002). The hardness behaviour of 2024-SiC was presented at the *Figure 2.12*. It can be seen that after 150 h of ageing, the base material reached to 112 HV. However, the composite reached 120 Hv which was 8 Hv higher than untreated sample. The benefic on the hardness of cryogenic heat treated 2024 was also

confirmed by the study of Padmini et al.(Padmini et al., 2019b). The hardness of 2024 reached to from 135 to 140 Hv.

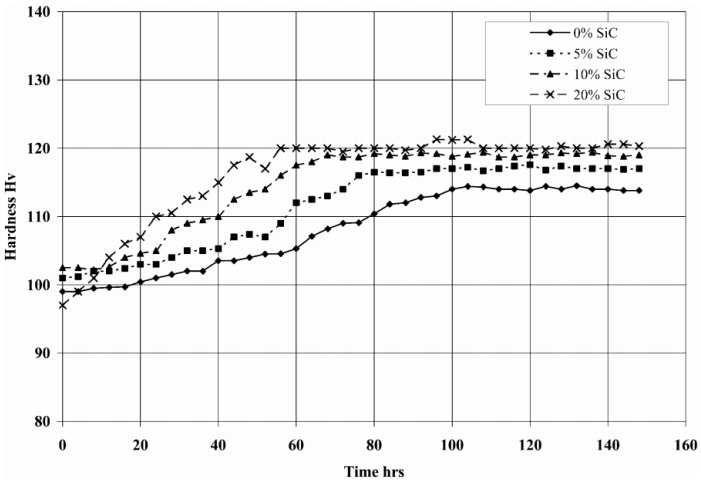

Figure 2.12. The hardness behaviour of composites (Bekheet et al., 2002).

On the other hand, 2026 aluminum alloy was subjected to tensile deformation and strain value was determined. An increase in the width of the sample, increased the strain concentration (Lam et al., 2010). Wang et al. examined the aged and deep cryogenic treated FSW joints of 2024-T351 aluminum alloy (Wang et al., 2014). They found that the yield stress, ultimate strength and elongation decreased after ageing and deep cryogenic heat treatment (*Figure 2.13*). Similar method was applied without cryogenic treatment to join 2024-T351 and 6056-T4 alloy (Amancio-Filho et al., 2008).

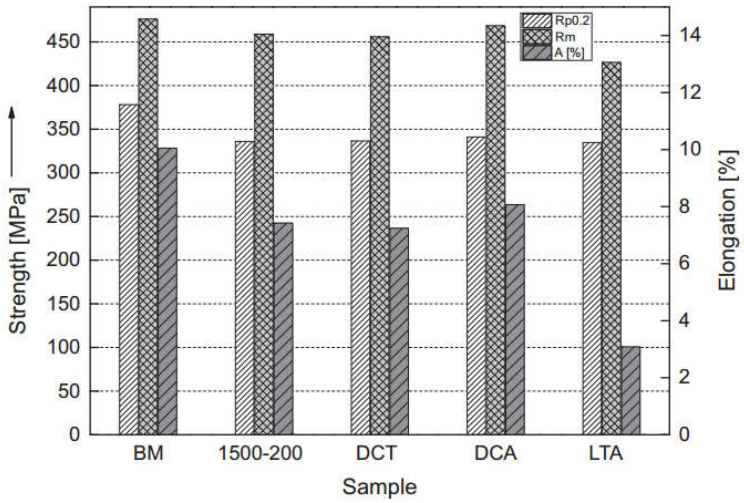

Figure 2.13. Tensile properties of 2024 with different heat treatment (Wang et al., 2014).

Moreover, the sample 2024 and 7075 subjected to the cryogenic heat treatment at -196 °C for 4h increased the yield strength 32 and 20 MPa and the tensile strength to 26 and 21 MPa (Faraji et al., 2018).

2.3.2 Mechanical performance of 6000 aluminum alloys

It is well documented that 6061 aluminum alloy had mild strength, heat treatable and good corrosion characteristic. The 6061 aluminum alloy is used in automotive and aviation industry to gain weight. The effect of ageing on the hardness was studied and they found that ageing at 180 °C for 24 h decreased the hardness from 105 Hv (180 °C for 11 h) to 95 Hv (Demir and Gündüz 2009).

Ozturk et al. also worked on the mechanical properties of 6061 alloys. They found that after 120 min of ageing at the temperature of 200 °C, a decrease of hardness value was observed as seen at *Figure 2.14* (Ozturk et al., 2010).

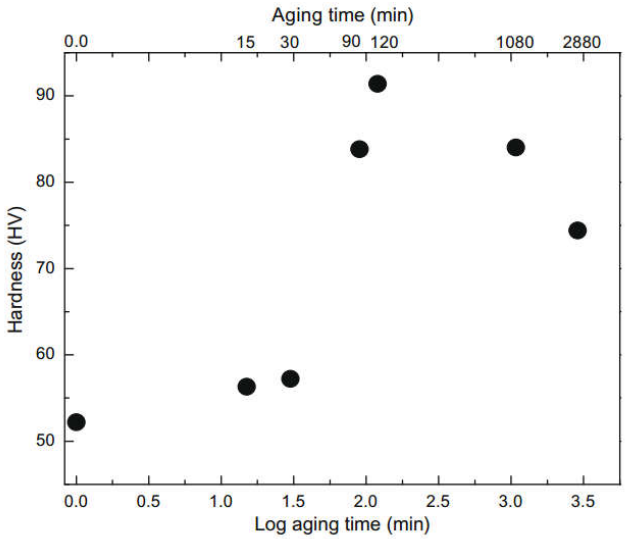

Figure 2.14.The hardness behavior with ageing time of the 6061 aluminum alloy (Ozturk et al., 2010).

According to the works realized, the T6 treatment lead β″ needle-shaped precipitates and the sequence of precipitation of Al-Mg-Si were given in the **Hata! Başvuru kaynağı bulunamadı.** (Maisonnette et al., 2011). Mariora et al. studied the effect of β″ phase on the hardness of 6xxx series of aluminum alloys (Marioara et al., 2006). In another study, the residual stress formed after cryogenic heat treatment to 6061 aluminum alloy was examined by Ko et al. (Ko et al., 2013).

Table 2.3. Al-Mg-Si composition of precipitate (Maisonnette et al., 2011).

Phase	Composition
GP zone	Mg_1Si_1
β″	Mg_5Si_6
β′	Mg_9Si_5
β	Mg_2Si

3. MATERIALS AND METHODS

3.1 Materials preparation

The aluminum untreated and treated 2024 and 6061 alloys in form of sheet were obtained by supplier and presented at the *Table 3.1*. Then the sheet metals were cut by using laser cutting machine to obtain tensile sample (ASTM 646-98) as given in the *Figure 3.1 and Table 3.2.*

Table 3.1. The treatment applied to the 2024 and 6061 aluminum alloy.

Aluminum Alloys	Treatment
2024-T0	Untreated
2024-T3	T3 heat treatment applied
6061-T0	Untreated
6061-T6	T6 heat treatment applied

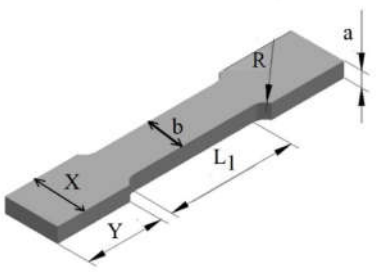

Figure 3.1. Tensil test specimen according ASTM 646-98.

Table 3.2. Dimension of tensile sample given at **Hata! Başvuru kaynağı bulunamadı.**

a	b	Y	X	R	L_1	L_2
3 mm	20 mm	35mm	30 mm	35 mm	83.76 mm	173.76 mm

3.2 Deep cryogenic heat treatment

Deep cryogenic heat treatment was performed at -196 °C with different period of time. Briefly, the prepared tensile samples were placed in the cryogenic furnace and then the furnace was heated at the rate of 5 °C/ min to -196 °C. Three soak time were set for cryogenic treatment 8 h, 16 h and 24 h. After desired waited time, the furnace was cool down to room temperature at the velocity of 5 °C/ min.

3.3 Mechanical test

The tensile test was carried out using Shimadzu AG-IS 250 kN (*Figure 3.2*) at the velocity of 2 mm/min according to ASTMD790. The results were presented as stress-strain curves. On the other hand, hardness measurement was realized by applying 5 gf on the surface of the sample for 10 s (*Figure 3.3*).

Figure 3.2. Tensile test apparatus.

Figure 3.3. Hardness measurement apparatus (2021).

3.4 Corrosion test

The corrosion tests were performed in the 3.5 wt.% NaCl solution at room temperature. For this purpose, a three electrode system was employed to test the samples. First electrode was assigned as working electrode, the second electrode which was Ag/AgCl reference electrode and the last electrode which is made of carbon was employed as counter electrode. For all experiment, the test begins after 15 min of immersion of the samples in the marine solution. The open circuit potential, potentiodynamic and electrochemical impedance spectroscopy (EIS) experiments were executed to study the corrosion performance of the samples

).

Figure 3.4. Corrosion apparatus.

4. RESULTS AND DISCUSSIONS

4.1 Mechanical results

4.1.1 Hardness Behavior

The hardness of the samples were measured and presented at the *Figure 4.1, Figure 4.2, Figure 4.3 and Figure 4.4.* For the sample 2024-T0, the hardness was decreased after performed cryogenic treatment. The value decreased from 58 HV (0h) to 55 HV (8h). Increasing the time of treatment decreased the hardness to 53 HV after 16 h. A slight increase was observed after 24h of treatment which was 54 HV (*Figure 4.1*).

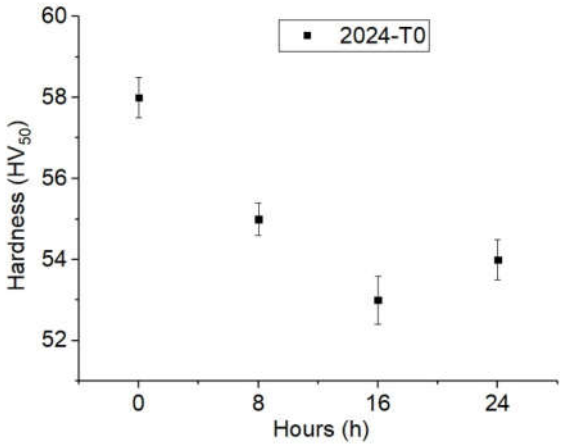

Figure 4.1. The hardness behaviour of untreated and treated 2024-T0.

On the other hand, the treatment of cryogenic treatment was benefic for the alloy 2024-T3. The hardness increased from 142 HV to 155 HV after 24 h of treatment (*Figure 4.2*).

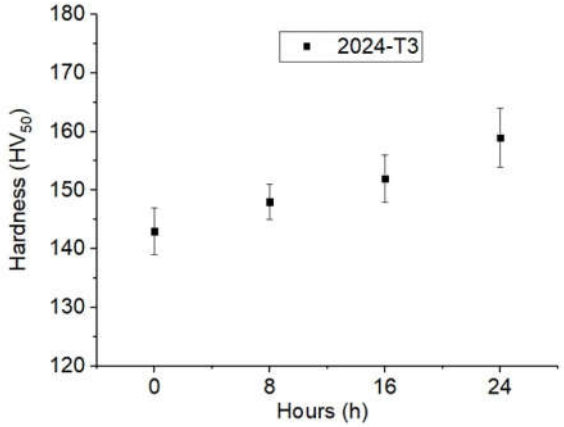

Figure 4.2. The hardness behaviour of untreated and treated 2024-T3.

The cryogenic treatment decreased the hardness of 6061-T0 after 8h of treatment from 42 HV to 41 HV. However, the treatment 16h and 24 lead a slight increase which reached maximum of 43 HV (*Figure 4.3*). While, the hardness increased from 115 HV to 127 HV after cryogenic treatment (*Figure 4.4*).

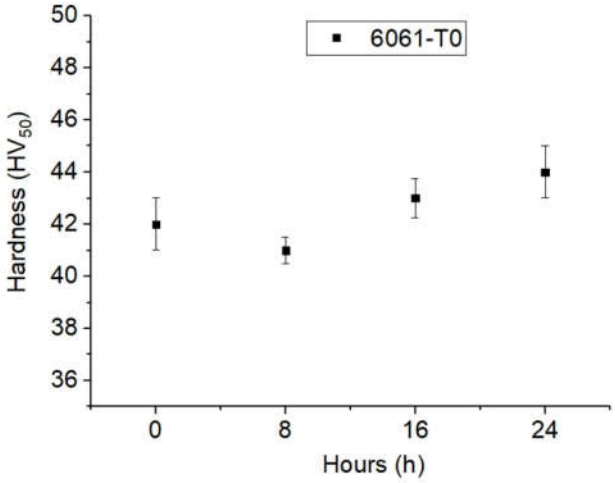

Figure 4.3. The hardness behaviour of untreated and treated 6061-T0.

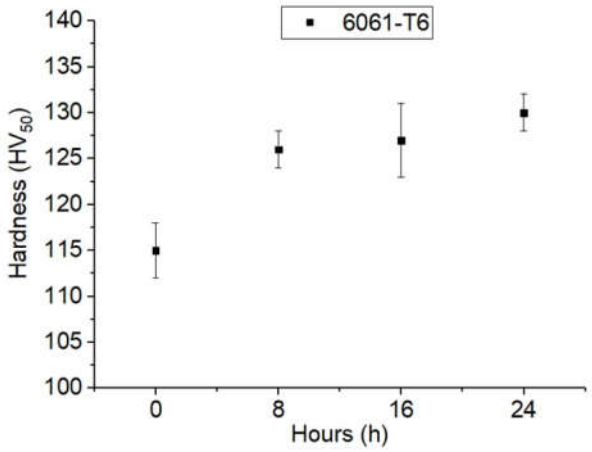

Figure 4.4. The hardness behaviour of untreated and treated 6061-T6.

4.1.2 Strain-Stress Behavior

Figure 4.5 shows the tensile behaviour and the *Figure 4.6* presents the extracted data from the tensile test of untreated and treated 2024-T0 aluminum alloy. As expected, all the samples conducted similar tensile curves. The UTS of untreated was 165 MPa which was higher than 2024-T0-16h (164 MPa) and lower than 2024-T0-8h (168 MPa) and 2024-T0-24h (166 MPa). Meanwhile, the elongation was lower for 2024-T0 with 23 % compared to other samples. Higher ductility behaviour was obtained when using short cryogenic treatment time with the sample 2024-T0-8h (25 %). On the other hand, the yield strength was higher for the sample 2024-T0-16h followed by 2024-T0, 2024-T0-8h and 2024-T0-24h. The energy absorption of the samples was also calculated which is defined as the total amount of energy absorbed before fracture. The lower and higher resistance against failure was recorded for 2024-T0 (33 J/cm3) and 2024-T0-8h (39 J/cm3), respectively. In general, it can be state here that the cryogenic treatment slightly improved the mechanical properties of 2024-T0 aluminum alloys.

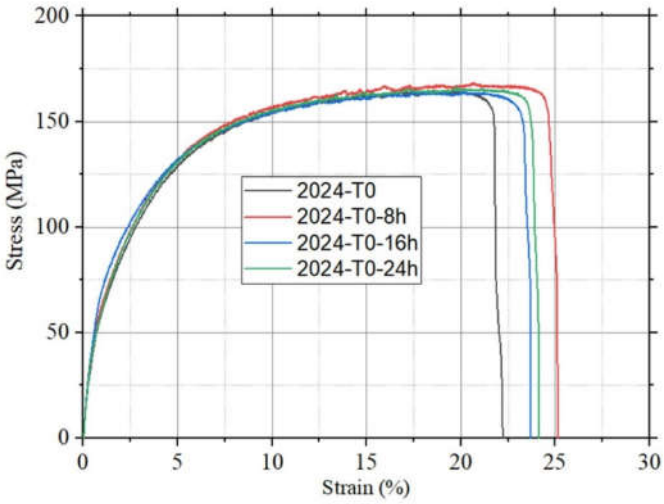

Figure 4.5. Tensile test results of untreated and treated 2024-T0 aluminum alloys.

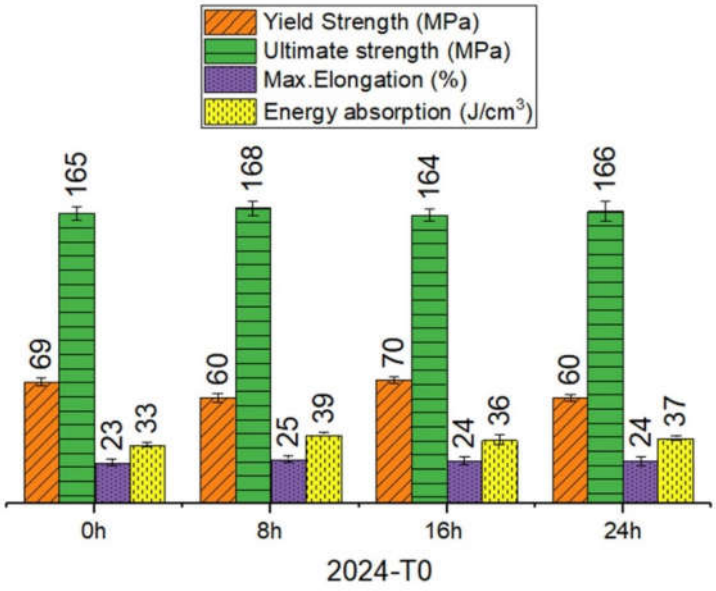

Figure 4.6. Data extracted from the *Figure 4.5*.

The alloy 2024-T3 which has better mechanical properties compared to 2024-T0 was subjected to deep cryogenic heat treatment to evolve the mechanical properties. The findings on the tensile behaviour was exhibited at the Figure 4.*7and* Figure 4.*8*. When regarding closely to the tensile behaviour of the untreated and treated sample 2024-T3, it can be concluding that they had similar trends. The highest ultimate tensile strength was acquired when applying low period

of cryogenic treatment, it reached to 469 MPa. Increasing the cryogenic heat treatment time decreased slowly the UTS compared to untreated 2024-T3. On the other hand, the yield strength was better for all cryogenic treatment time and it attained maximum 364 MPa when applying 24 h. Regarding to elongation, it was noticed that the samples 2024-T3 had lower ductility compared to 2024-T0. Meanwhile, the resistance against failure was enhanced with the treatment of 8 h and it increased from 93 J/cm3 to 98 J/cm3.

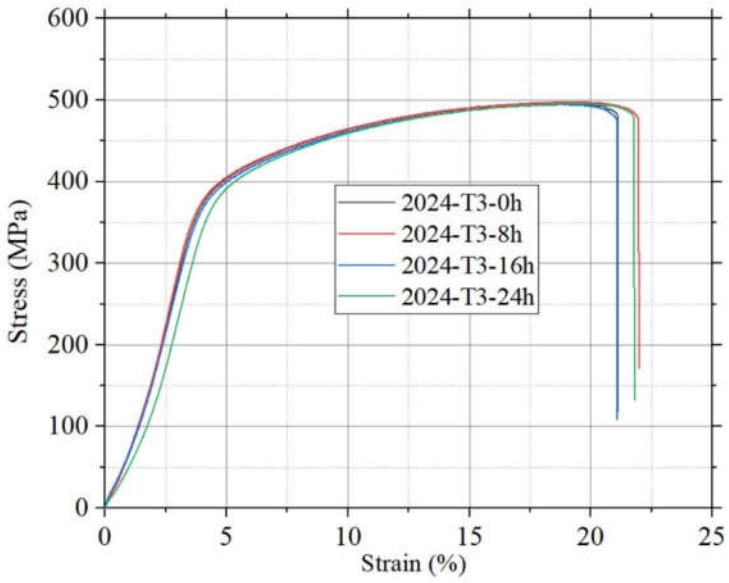

Figure 4.7. Tensile test results of untreated and treated 2024-T3 aluminum alloys.

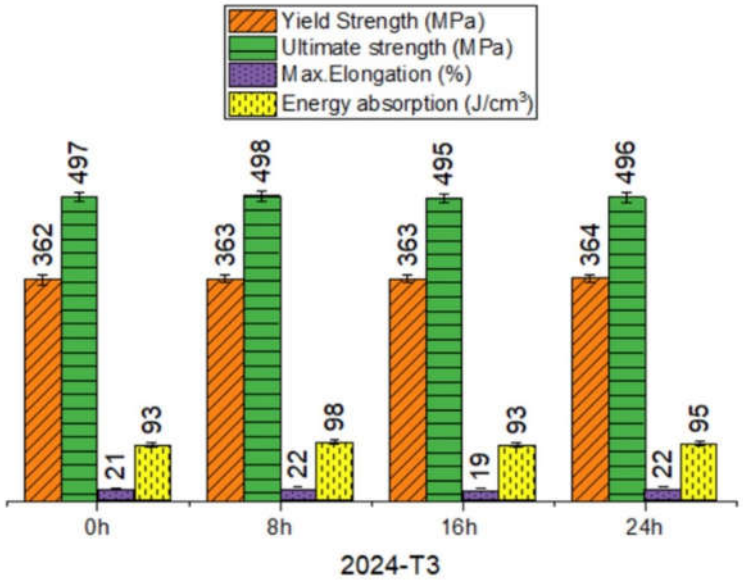

Figure 4.8. Data extracted from *Figure 4.7*.

The results of untreated and treated 6061-T0 and 6061-T6 was presented at *Figure 4.9, Figure 4.10, Figure 4.11and Figure 4. 12.*

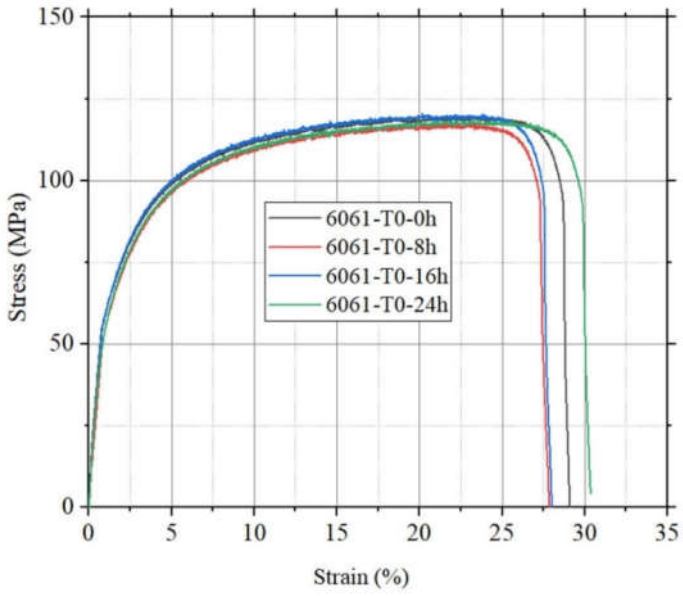

Figure 4.9. Tensile test results of untreated and treated 6061-T0 aluminum alloys.

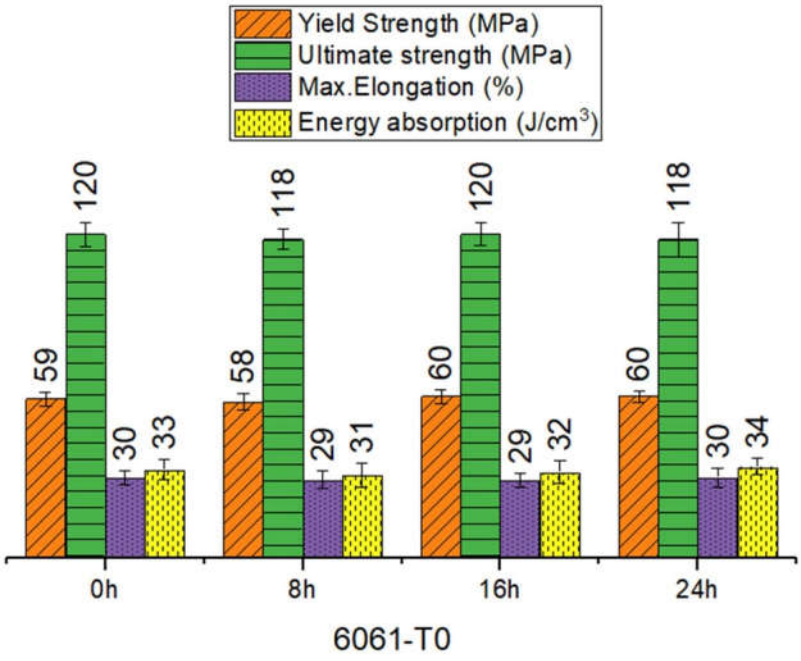

Figure 4.10. Data extracted from *Figure 4.9*.

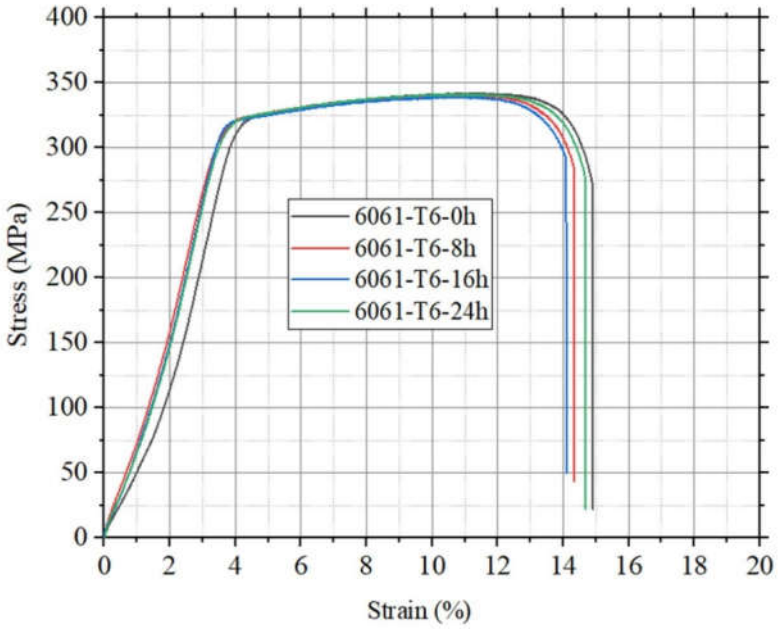

Figure 4.11. Tensile test results of untreated and treated 6061-T6 aluminum alloys.

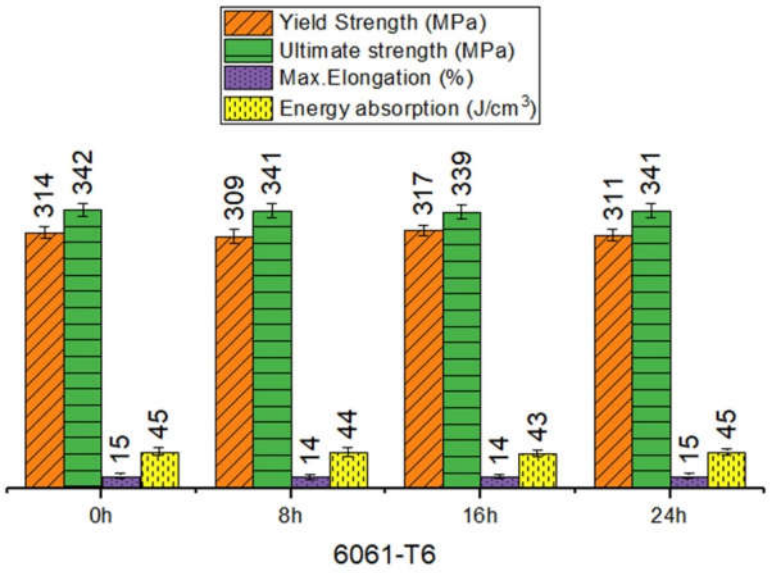

Figure 4. 12. Data extracted from *Figure 4.11*.

4.2 Electrochemical results

4.2.1 Ecorr vs time

The free corrosion potential behavior of untreated and treated 2024-T0 alloy in the 3.5 wt. % NaCl was presented in the **Hata! Başvuru kaynağı bulunamadı.**At first glance, it can be seen that all samples finished around -720 mV after 1 h of immersion. However, the sample 2024-T0-8h was behaved cathodic compared to other alloys during the test. In opposition, the treated alloy 2024-T0-16h and 2024-T0-24h had similar OCP trend as 2024-T0-0h.

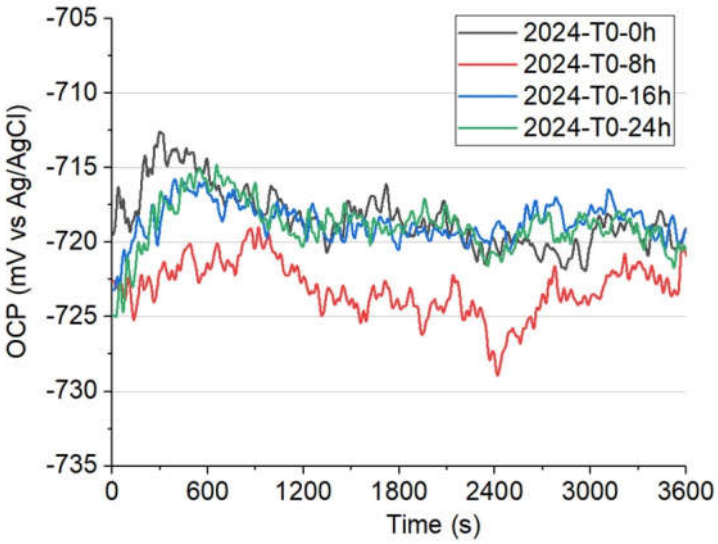

Figure 4.13. The open circuit potential behaviour of untreated and treated 2024-T0 alloy.

The OCP performance of the 2024-T3 was screened at the Figure 4.*14*. In general, the untreated sample was more anodic compared to treated sample. In adverse, the OCP of the sample 2024-T3-8h performed more cathodic after 0.3 h of the test. On the other hand, the OCP of the samples ended around -615 mV after immersion of 1 h.

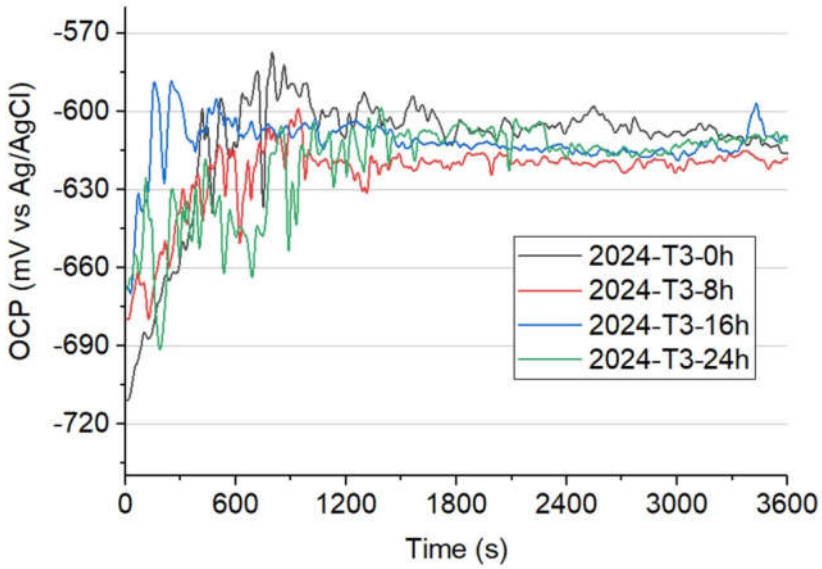

Figure 4.14. The open circuit potential behaviour of untreated and treated 2024-T3 alloy.

The free corrosion potential of untreated and treated 6061-T0 was measured and presented at Figure 4.*15*. At first glance, it was observed that the OCP value of the original sample begin at -780 mV which was more cathodic and stayed constant after half hour compared to treated samples. In opposite, the treated sample started more anodic compared to untreated sample and the free corrosion potential finished around -720 mV for all treated samples.

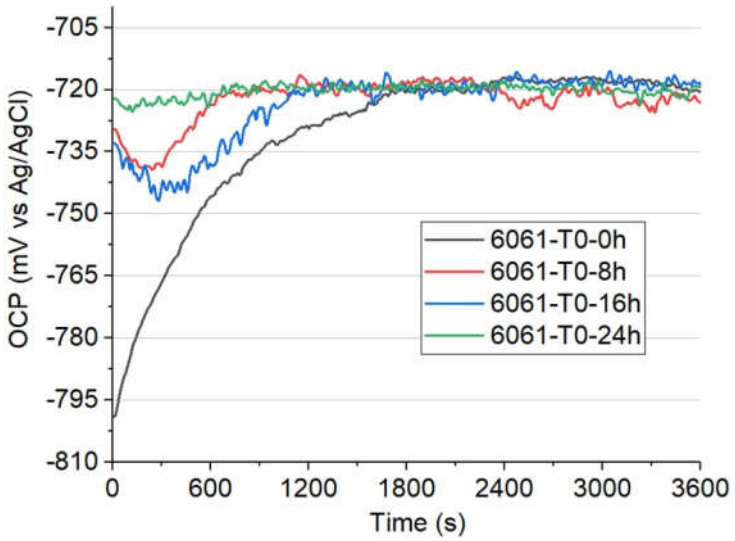

Figure 4.15. The open circuit potential behaviour of untreated and treated 6061-T0 alloy.

On the other hand, the free corrosion potential tendency of 6061-T6 was also investigated in the 3.5 wt.% NaCl. The findings show that the cryogenic heat treated 6061-T6-8h had slightly higher anodic potential compared to other samples Figure 4.*16*. Although, the corrosion potential of 6061-T6-24h started more anodic approximately -715 mV, it finished more anodic with -730 mV.

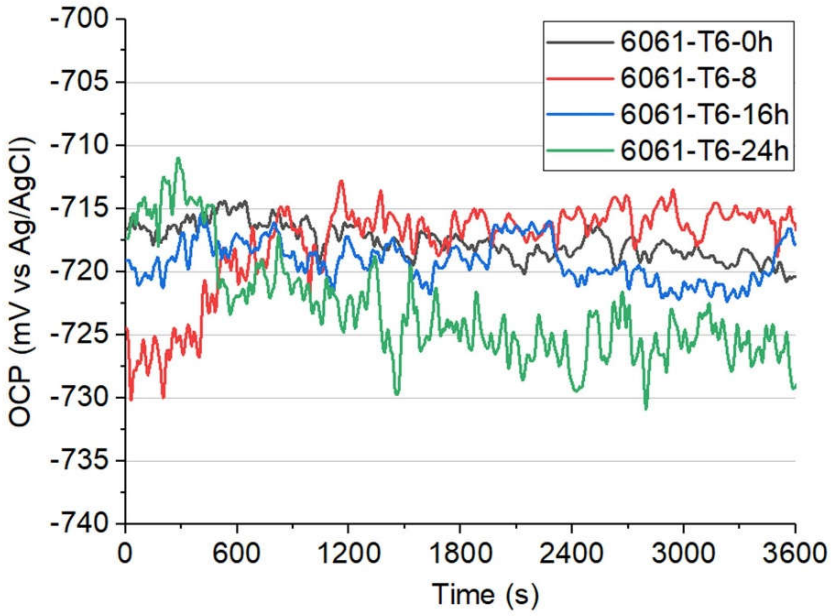

Figure 4.16. The open circuit potential behaviour of untreated and treated 6061-T6 alloy.

4.2.2 Passivation behavior analysis

The polarisation curves of untreated and treated alloy 2024-T0 was presented at Figure 4.*17*. At first glance, it can be seen a passivation zone for all sample in the branch of anodic curves indicating of formation of oxide film. This passivation area was bigger for 2024-T0-0h followed by 2024-T0-16h, 2024-T0-8h and 2024-T0-24h, respectively. The corrosion potential, corrosion current and corrosion rate of samples were obtained from Tafel curves and presented at the Table 4.*1*. Although, the corrosion potential of untreated sample was found -982 mV which was higher than 2024-T0-8h and 2024-T0-24h, the corrosion current as well as corrosion rate was lower than rivals.

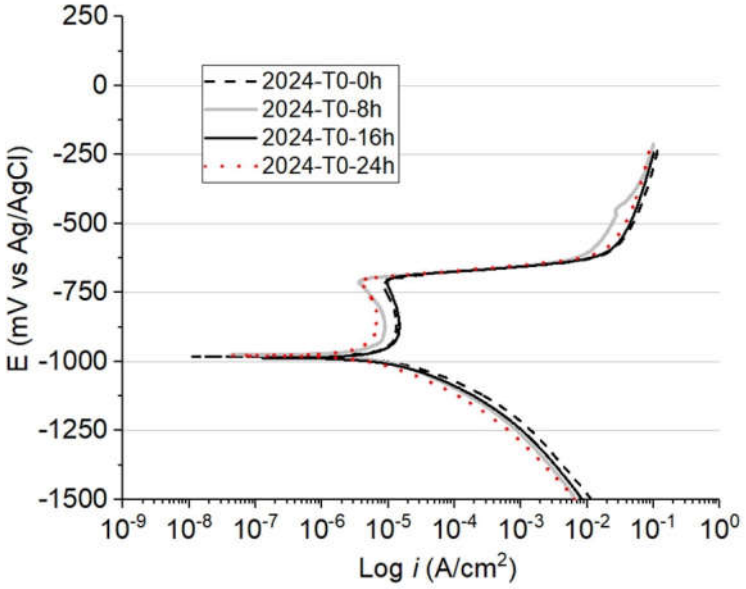

Figure 4.17. Potentiodynamic curves of untreated and treated 2024-T0.

Table 4.1. Data extracted from *Figure 4.17*.

	Beta A (V/decade)	Beta C (V/decade)	Icorr (uA)	Ecorr (mV)	Corrosion rate (mpy)
2024-T0-0h	53,80e-3	33,70e-3	3,270	-982,0	4,151
2024-T0-8h	31,06e3	121,0e-3	13,80	-975,0	17,45
2024-T0-16h	10,50e3	118,6e-3	19,10	-987,0	24,26
2024-T0-24h	659,8e-3	87,30e-3	5,690	-978,0	7,213

Otherwise, the polarisation curves of untreated and treated alloy 2024-T3 had similar behaviour as 2024-T0 (Figure 4.*18* and Figure 4.*19*). The passivation area was higher for 2024-T3-24h (-920 mV to – 600 mV) followed by 2024-T3-8h (from -885 mV to -625 mV), 2024-T3-16h (from -910 mV to -606 mV) and 2024-T3-0h (from -866mV to -664 mV) (Table 4.*2*). It can be state here that the cryogenic treated samples had better resistance of oxide film compared to untreated sample. Moreover, the corrosion potential measured was for 2024-T3-0h, 2024-T3-8h and 2024-T3-24h was -1000 mV while it was -997 mV slightly more anodic for 2024-T3-16h. Furthermore, the corrosion rate was higher for the untreated sample with 16.54 mpy which was 3.5 times higher than 2024-T3-16h.

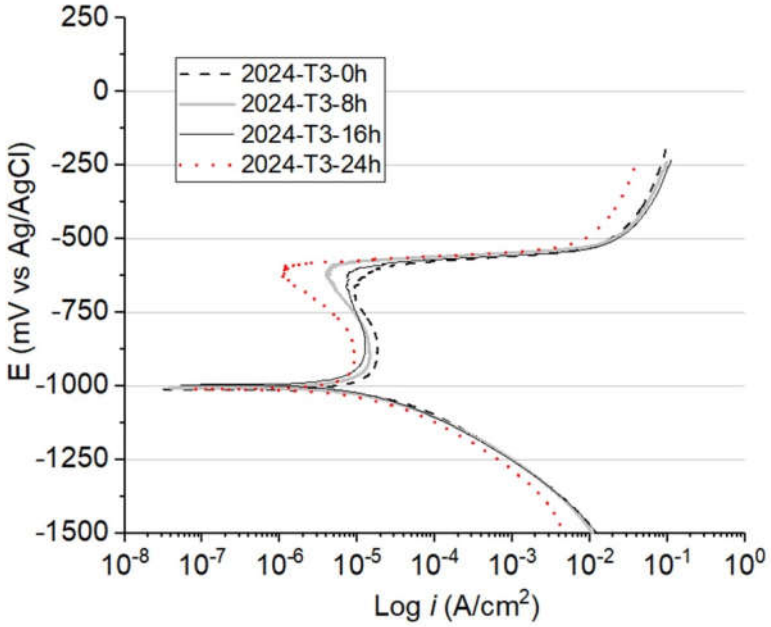

Figure 4.18. Potentiodynamic curves of untreated and treated 2024-T3.

Table 4.2. Data extracted from *Figure 4.18*.

	Beta A (V/decade)	**Beta C (V/decade)**	**Icorr (uA)**	**Ecorr (mV)**	**Corrosion Rate (mpy)**
2024-T3-0	392,9e-3	72,40e-3	13,00	-1000	16,45
2024-T3-8	105,0e-3	43,80e-3	4,220	-1000	5,354
2024-T3-16	102,0e-3	54,20e-3	3,660	-997	4,638
2024-T3-24	1,000e15	85,80e-3	10,70	-1000	13,61

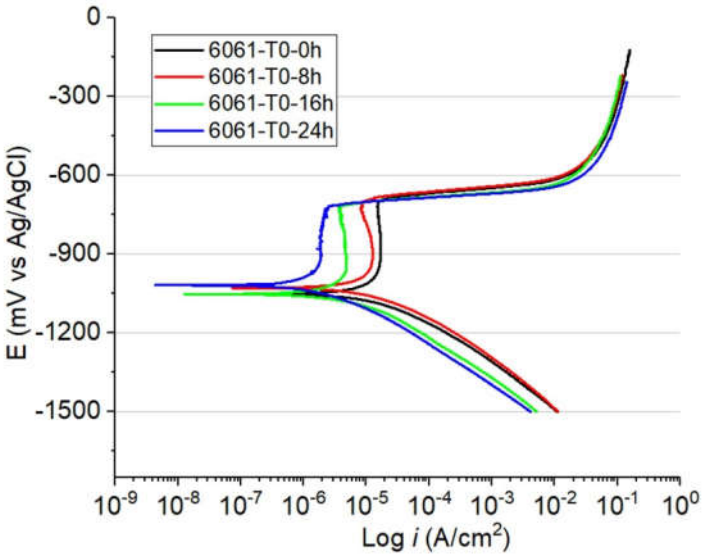

Figure 4.19. Potentiodynamic curves of untreated and treated 6061-T0.

The anodic polarisation curves of untreated and treated 6061-T0 exhibited passivation in the 3.5 wt. % NaCl solution (*Figure 4.19*). The corrosion potential was found lower for the sample 6061-T0-24h which was -1020 mV (Table 4.*3*). However, the corrosion potential of 601-T0-0h and 6061-T0-16h were equal. Although, the corrosion potential was higher for 6061-T0-16h, the Icorr as well as the corrosion rate was found 1.88 uA and 2.39 mpy lower than original sample.

Table 4.3. Data extracted from *Figure 4.19*.

	Beta A (V/decade)	**Beta C (V/decade)**	**I_{corr} (uA)**	**E_{corr} (mV)**	**Corrosion Rate (mpy)**
6061-T0-0h	622,8e-3	131,0e-3	15,60	-1050	19,84
6061-T0-8h	276,2e-3	96,60e-3	8,82	-1030	11,18
6061-T0-16h	153,6e-3	55,20e-3	1,88	-1050	2,391
6061-T0-24h	841,4	179,9e-3	3,58	-1020	4,542

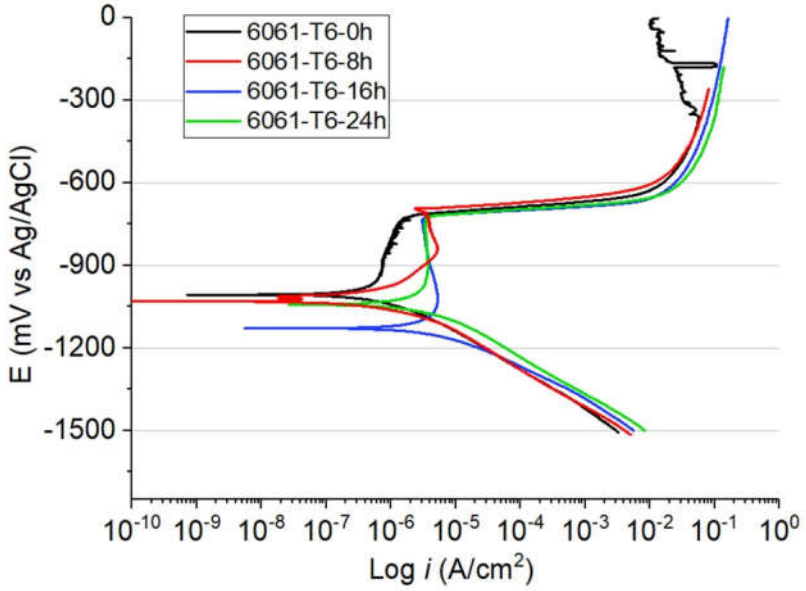

Figure 4.20. Potentiodynamic curves of untreated and treated 6061-T6.

The T6 treated 6061 was also investigated to find the effect of the cryogenic treatment. At first look, it can be state here that a passivation zone was observed for all sample as observed for 6061-T0 (Figure 4.*20*). Besides, it appears that the treated sample had more cathodic corrosion potential than untreated sample; it was found for -1010 mV for untreated sample. However, the corrosion rate and the corrosion current was found lower for the sample 6061-T6-8h and higher for the sample 6061-T6-24h (Table 4. *4*)

Table 4. 4. Data extracted from *Figure 4.20*.

	Beta A (V/decade)	**Beta C (V/decade)**	**Icorr (uA)**	**Ecorr (mV)**	**Corrosion Rate (mpy)**
6061-T6-0h	116,0e-3	51,30e-3	290,0 nA	-1010	368,4e-3
6061-T6-8h	1,000e15	10,50e-3	13,50 nA	-1030	19,40e-3
6061-T6-16h	80,90e-3	42,10e-3	1,350 uA	-1130	1,710
6061-T6-24h	151,9e-3	60,30e-3	1,540 uA	-1040	1,952

4.2.3 Electrochemical Impedance Spectroscopy (EIS)

The Nyquist plots of untreated and treated 2024-T0 were shown at Figure 4.*21*. At first glance, it can be deducing that a semi-circle capacitive loop, inductive loop and a Warburg impedance curves were located. At high frequency, the sample 2024-T0-8h had bigger semi-circle diameter meaning better resistance of oxide film. The inductive loop at low frequency which is attributed to adsorption of materials to the surface such as corrosion products was also higher for 2024-T0-8h sample. Furthermore, the untreated sample exhibited poor corrosion resistance compared to cryogenically treated sample. The Warburg resistance which is also named diffusion of ions from the metal surface to the solution or contrary consume the electrons, was observed on the 2024-T0-16h. This finding also fitting why high corrosion rate found after anodic polarisation for 2024-T0-16h at the Table 4.*5*. The equivalent electric circuit was adapted to the Nyquist curves and the results were given at the Table 4.*5* and Figure 4.*22*.

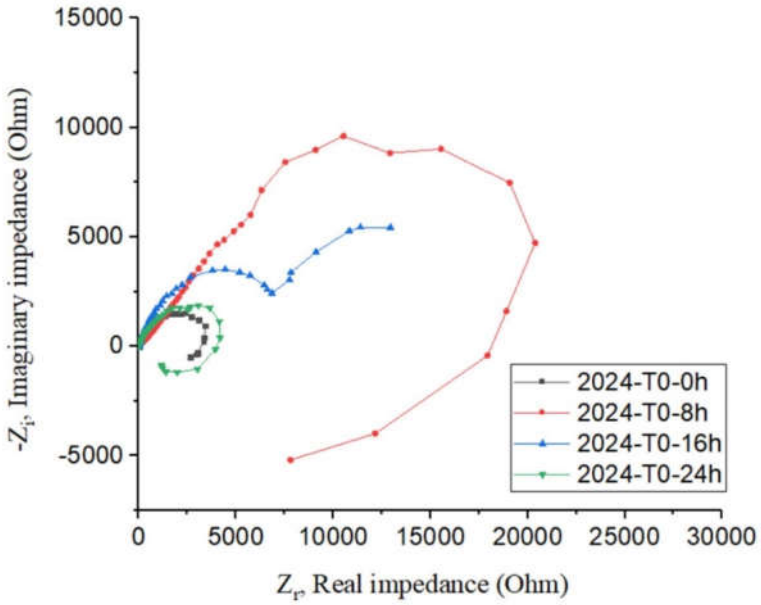

Figure 4.21. The Nyquist plot of untreated and treated sample 2024-T0.

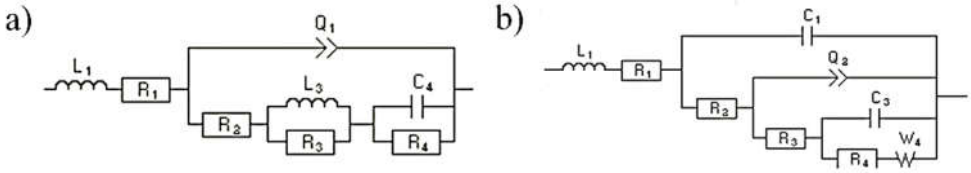

Figure 4.22. The equivalent electric circuit of untreated and treated 2024-T0.

Table 4.5. Data extracted after fitting the Nyquist curves showing equivalent electric circuit.

	L1 (H)	R1 (Ohm)	Q1 (F.s^(a-1))	a1	R2 (Ohm)	L3 (H)	R3 (Ohm)	C4(F)	R4(Ohm)
2024-T0-0h	-2,56E-06	12,54	4,21E-05	0,926 3	3 635	-169	-1 666	-1,49E-03	1,04E+16
2024-T0-8h	2,85E-03	-577,7	8,01E-05	0,353 3	-4,86E+06	-3,24E+06	4,84E+06	-0,138 2e-6	4,87E+06
2024-T0-24h	-1,70E-03	23,71	1,01E-05	1	3 565	-405,7	-3 252	1,98E-05	557,2
	R1 (Ohm)	**C1 (F)**	**R2 (Ohm)**	**Q2 (F.s^(a-1))**	**a1**	**R3 (Ohm)**	**C3 (F)**	**R4 (Ohm)**	**S4 (Ohm.s^-1/2)**
2024-T0-16h	101,2	3,74E-05	7 028	-0,031 53	0,512	13 747	-4,86E-09	-13 750	23,16

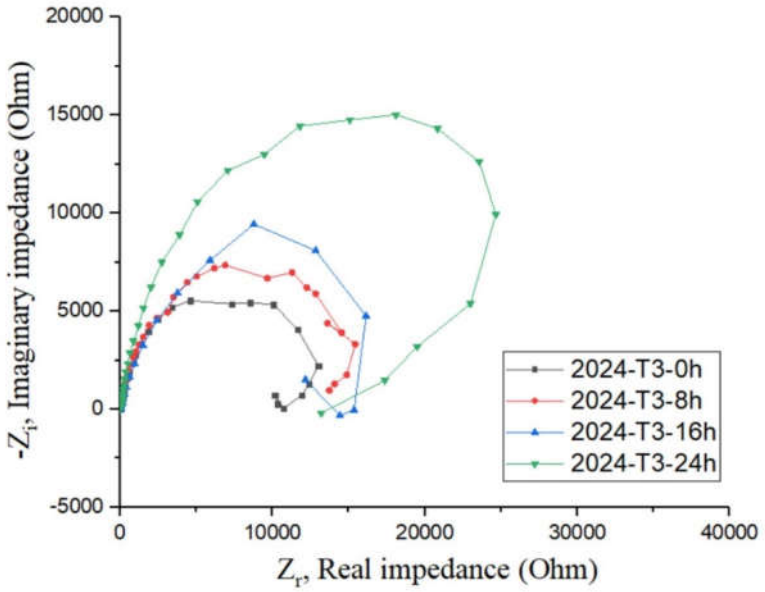

Figure 4.23. The Nyquist plot of untreated and treated sample 2024-T3.

The corrosion resistance of 2024-T3 was also evaluated and it was seen a semi-circle capacitive loop and inductive loop for all sample (Figure 4.*23 and* Table 4.*6*). The impedance resistance was higher for the sample 2024-T3-24h followed by 2024-T3-16h, 2024-T3-8h and 2024-T3-0h. From these findings, it can be deducing that the cryogenic treatment increased the

corrosion resistance. The inductive loop at low frequency as observed for the sample 2024-T0, it is due to the adsorption of the corrosion products on the surface. The equivalent electric circuit of untreated and treated 2024-T3 was presented at Figure 4.*24*.

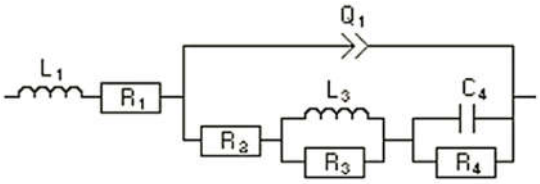

Figure 4.24. The equivalent electric circuit of untreated and treated 2024-T3.

Table 4.6. Data extracted after fitting the Nyquist curves showing equivalent electric circuit.

	L1 (H)	R1 (Ohm)	Q1 (F.s^(a-1))	a1	R2 (Ohm)	L3 (H)	R3 (Ohm)	C4(F)	R4(Ohm)
2024-T3-0h	-0,122 6e-3	15,73	7,12E-06	1	2 664	-42,5	-1 877	1,00E-05	9 778
2024-T3-8h	-3,74E-06	39,09	1,92E-05	0,958 4	17 263	488,9	-2 113	-8,34E-08	-1 164
2024-T3-16h	-0,476 8e-3	106,6	3,96E-03	0,999 8	-112 132	1,40E+06	-18 821	-7,91E-18	130 953
2024-T3-24h	1,79E-03	145,7	7,30E-06	1	27 408	-1 321	2 300	0,113 2e-3	-6 683

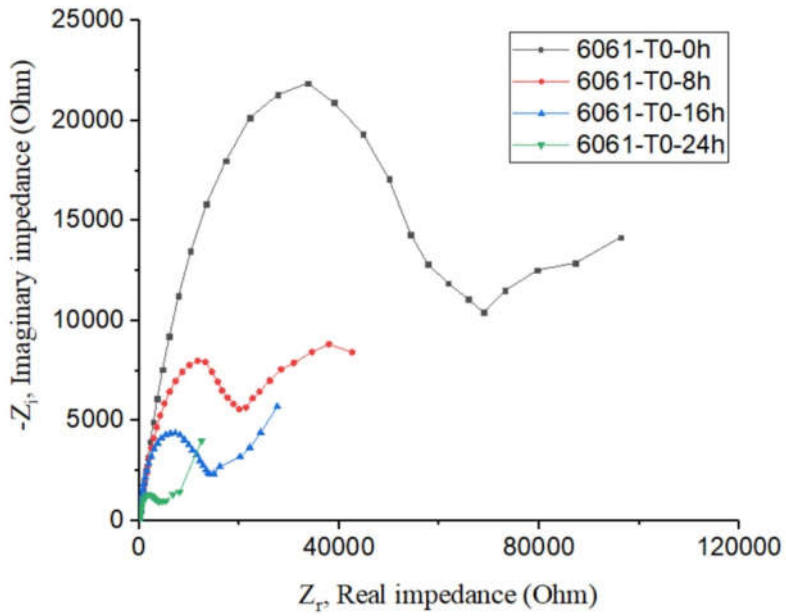

Figure 4.25. The Nyquist plot of untreated and treated sample 6061-T0.

On the other hand, the cryogenic treatment decreased the corrosion resistance of 6061-T0. However, at high frequency a semi-circle capacitive loop and a Warburg effect was observed

for all samples (Figure 4.*25*). The Warburg effect as mentioned above, mass diffusion on the surface of electrode such as products species or soluble reactant were the main reason. The equivalent electrical circuit (Figure 4.*26*) and the data extracted from the fitting curves were given at the Table 4.*7*.

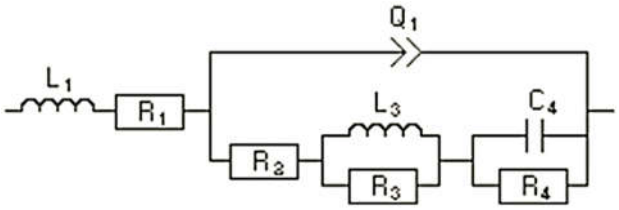

Figure 4.26. The equivalent electric circuit of untreated and treated 6061-T0.

Table 4.7. Data extracted after fitting the Nyquist curves showing equivalent electric circuit.

	L1 (H)	R1 (Ohm)	C1 (F)	R2 (Ohm)	Q2 (F.s^(a-1))	a1	R3 (Ohm)	C3 (F)	R4 (Ohm)	W4 (Ohm.s^-1/2)
6061-T0-0h	-1,41E-05	448,1	1,35E-05	-74 354	8,89E-06	0,081 22	2,91E+06	6,38E-06	656 598	-295 394
6061-T0-8h	-0,497 3e-3	403,7	8,21E-05	17 729	-0,023 25	0,511 9	-7 073	-1,60E-06	7 066	32
6061-T0-16h	-9,02E-06	131,8	7,03E-05	5 849	0,275 9e-3	0,338 2	3,61E+06	-4,86E-09	-3,58E+06	-4 828
6061-T0-24h	-2,65E-05	86,05	0,277 7e-3	3 424	-0,078 24	0,503 9	-1 283	-1,11E-05	1 282	9,115

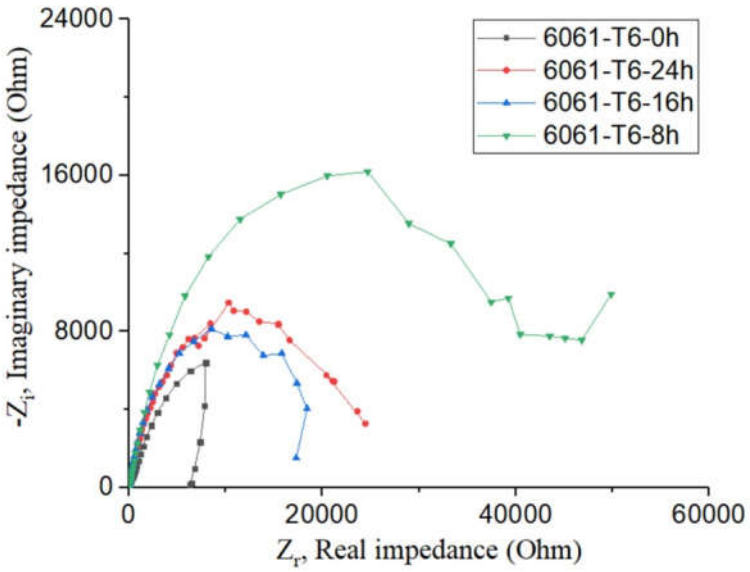

Figure 4.27. The Nyquist plot of untreated and treated sample 6061-T6.

When regarding to the sample 6061-T6, the cryogenic treated sample were more resistant against the untreated sample (Figure 4.*27*). The 6061-T6-8h treated sample had better corrosion resistance followed by 6061-T6-24h, 6061-T6-16h and 6061-T0-0h. Furthermore, semi-circle capacitive loop and Warburg effect was observed for the sample 6061-T0-8h. This result was not surprise because, it was found that the corrosion rate as well as corrosion current was lower for the sample 6061-T0-8h compared to other samples (*Figure 4. 28*). Moreover, the Nyquist curves were fitted to find the equivalent electric circuit of untreated and treated 6061-T6 (**Hata! Başvuru kaynağı bulunamadı.**). The electrical circuit was consisted of L1 and L3 which corresponding to the electrolyte, R1, R2 and R3 to the resistance of the electrode and C to the capacitor for the sample 6061-T6-24h, 6061-T6-16h and 6061-T0-0h. While the W in the electrical circuit represent the Warburg effect for 6061-T6-8h sample. The data obtained from the equivalent electrical circuit was given at the (Table 4.*8*).

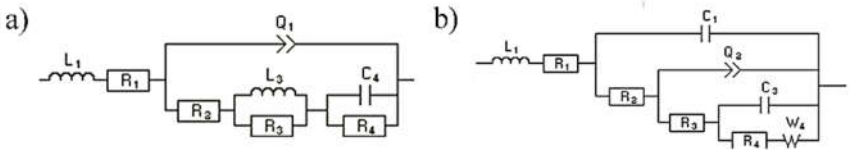

Figure 4. 28. The equivalent electric circuit of untreated and treated 6061-T6.

Table 4.8. Data extracted after fitting the Nyquist curves showing equivalent electric circuit.

	L1 (H)	R1 (Ohm)	Q1 (F.s^(a-1))	a1	R2 (Ohm)	L3 (H)	R3 (Ohm)	C4(F)	R4(Ohm)	
6061-T6-0h	6,02E-06	4,361	1,33E-05	0,691 2	21 723	-459,7	-15 692	1,58E-06	-767,2	
6061-T6-16h	-6,12E-06	20,69	4,14E-06	1	15 691	-2 454	-14 788	8,91E-06	2 501	
6061-T6-24h	-0,116 5e-3	39,45	2,05E-05	0,832 9	1,03E+06	2 161	-2 589	-5,16E-11	-1,01E+06	
	L1 (H)	**R1 (Ohm)**	**C1 (F)**	**R2 (Ohm)**	**Q2 (F.s^(a-1))**	**a1**	**R3 (Ohm)**	**C3 (F)**	**R4 (Ohm)**	**W4 (Ohm.s^-1/2)**
6061-T6-8h	-8,32E-06	8,85E+01	7,51E-06	5 702	3,17E-05	1,13E-01	2 874	7,16E-06	432 882	-202 886

5. CONCLUSIONS AND RECOMMENDATIONS

In this work, the aluminum alloy 2024-T0, 2024-T3, 6061-T0 and 6061-T6 were cryogenic treated to increase their mechanical and corrosion properties. The following findings was found;

- The hardness decreased for the alloy 2024-T0 after cryogenic treatment; the lowest hardness was 53 HV with 16 h treatment compared to 58 HV with 0 h. In adverse, the treatment increased the hardness for the alloy 2024-T3 from 142 HV to 155 HV after 24h.

- Although, the treatment decreased the hardness of 6061-T0 after 8 h of treatment, it was observed a slight increase after 16 h of treatment which reached maximum of 43 HV. On the other hand, the treatment leads an increment for the alloy 6061-T6 which attain 129 HV after 24 h compared to 115 HV for 0 h.

- The crypgenic treatment increased slightly the mechanical properties of the alloy 2024-T0, especially the elongation and energy absorption. The higher elongation and energy absorption was obtained with the sample 2024-T0-8h.

- Regarding to the sample 2024-T3, the yield strength and energy absorption was slightly improved after cryogenic treatment. Furthermore, the UTS and elongation was higher for the sample 2024-T3-8h.

- Although, the yield strength of the alloy 6061-T0 was improved after treatment. On the other hand, the yield strength of the alloy 6061-T6 decreased after cryogenic treatment except for the 16h of treatment. Moreover, the UTS decreased from 342 MPa to 339 MPa after treatment for the 6061-T6.

- The energy absorption of the alloy was enhanced for the alloy 6061-T0 which reached 34 J/cm^3 after 24 h of treatment.

- The free corrosion potential of untreated and treatead 2024-T0 had around -720 mV after immersion in the 3.5 wt. %NaCl solution. While the untreated and treated sample 2024-T3 finished more anodic with -615 mV.

- When looking the sample 6061-T0, the treated sample was more anodic compared to untreated sample during first 0.5 h but all the sample finished around -720 mV. On the other hand, the alloy 6061-T6-8h was outperformed compared to other sample with -715 mV.

- The corrosion current and the corrosion rate was found lower for untreated 2024-T0 compared to treated sample after Tafel analysis. In addition, the passivation zone was larger than for the sample 2024-T0 compared to rivals. The alloy 2024-T3 treated with cryogenic treatment had better corrosion resistance in term of the formation of protective oxide film when comparing the passivation area, corrosion current and corrosion rate.

- The treated alloy 6061-T0-24 performed better corrosion rate with 4.54 mpy and lower corrosion potential with -1020 mV. On the other hand, the corrosion current was lower for the alloy 6061-T0-16h compared to other alloys.

- A passivation zone was observed for the alloy untreated and treated 6061-T0 and 6061-T6: it can be state that the alloy 6061-T6-8h had lower corrosion current and corrosion rate compared to 6061-T6 alloys.

- The EIS findings showed that the alloy 2024-T0-8h had larger semi-circle than other sample meaning better resistance of oxide film. Otherwise, 2024-T0-16h exhibited Warburg resistance. Secondly, the alloy 2024-T3-24h performed higher resistance followed by 2024-T3-16h, 2024-T3-8h and 2024-T3-0h.

- All the sample of 6061-T0-0h displayed a semi-circle and Warburg resistance; the alloy 6061-T0-0h performed better while the alloy 6061-T0-24h exhibited lower corrosion resistance compared to other sample.

- The EIS results presented for the alloy 6061-T6 showed that the sample 6061-T6-8h performed better corrosion resistance followed by 6061-T6-24h, 6061-T6-16h and 6061-T0-0h.

- In general, it can be conclude that the cryogenic treatment was benefic for the alloy 2024-T3 and 6061-T6 alloy.

REFERENCES

Hardness tester. Availabe online: http://www.teskon.com/sertlik-universal-cihazi-urun943.html (accessed on 2021).

Amancio-Filho, S.T., Sheikhi, S., dos Santos, J.F., Bolfarini, C., 2008, Preliminary study on the microstructure and mechanical properties of dissimilar friction stir welds in aircraft aluminium alloys 2024-T351 and 6056-T4. Journal of Materials Processing Technology, 206(1): 132-142, doi:https://doi.org/10.1016/j.jmatprotec.2007.12.008.

Bekheet, N.E., Gadelrab, R.M., Salah, M.F., Abd El-Azim, A.N., 2002, The effects of aging on the hardness and fatigue behavior of 2024 Al alloy/SiC composites. Materials & Design, 23(2): 153-159, doi:https://doi.org/10.1016/S0261-3069(01)00072-3.

Chen, P., Malone, T., Bond, R., Torres, P., 2001, Effects of Cryogenic Treatment on the Residual Stress and Mechanical Properties of an Aerospace Aluminum Alloy.

Cole, G.S., Sherman, A.M., 1995, Light weight materials for automotive applications. Materials Characterization, 35(1): 3-9, doi:https://doi.org/10.1016/1044-5803(95)00063-1.

Committee, A.I.H., 1990, ASM Handbook: Properties and selection, ASM International:

Dasquet, J.P., Caillard, D., Conforto, E., Bonino, J.P., Bes, R., 2000, Investigation of the anodic oxide layer on 1050 and 2024T3 aluminum alloys by electron microscopy and electrochemical impedance spectroscopy. Thin Solid Films, 371: 183-190, doi:10.1016/S0040-6090(00)01016-6.

Deepa, P., Padmalatha, R., 2017, Corrosion behaviour of 6063 aluminium alloy in acidic and in alkaline media. Arabian Journal of Chemistry, 10: S2234-S2244, doi:https://doi.org/10.1016/j.arabjc.2013.07.059.

REFERENCES (continued)

Demir, H., Gündüz, S., 2009, The effects of aging on machinability of 6061 aluminium alloy. Materials & Design, 30(5): 1480-1483, doi:https://doi.org/10.1016/j.matdes.2008.08.007.

Dursun, T., Soutis, C., 2014, Recent developments in advanced aircraft aluminium alloys. Materials & Design (1980-2015), 56: 862-871, doi:https://doi.org/10.1016/j.matdes.2013.12.002.

Elango, G., Raghunath, B., Thamizhmaran, K., 2014, Effect of Cryogenic Treatment on Microstructure and Micro Hardness of Aluminium (LM25) - SiC Metal Matrix Composite. Journal of Engineering Research, 11: 64-68, doi:10.24200/tjer.vol11iss1pp64-68.

Fahimpour, V., Sadrnezhaad, S.K., Karimzadeh, F., 2012, Corrosion behavior of aluminum 6061 alloy joined by friction stir welding and gas tungsten arc welding methods. Materials & Design, 39: 329-333, doi:https://doi.org/10.1016/j.matdes.2012.02.043.

Faraji, F., VAHDAT, S.E., Nazarian, H., 2018, Effect of Deep Cryogenic Treatment on Precipitation Hardening of Aluminum 2024 and 7075. METALLURGICAL ENGINEERING, 21(3 (71) #T001080): -.

Franco Steier, V., Ashiuchi, E., Reißig, L., Araújo, J., 2016, Effect of a Deep Cryogenic Treatment on Wear and Microstructure of a 6101 Aluminum Alloy. Advances in Materials Science and Engineering, 2016: 1-12, doi:10.1155/2016/1582490.

Huang, Y., Shih, H., Huang, H., Daugherty, J., Wu, S., Ramanathan, S., Chang, C., Mansfeld, F., 2008, Evaluation of the corrosion resistance of anodized aluminum 6061 using electrochemical impedance spectroscopy (EIS). Corrosion Science, 50(12): 3569-3575, doi:https://doi.org/10.1016/j.corsci.2008.09.008.

REFERENCES (continued)

Jovičević-Klug, P., Podgornik, B., 2020, Review on the Effect of Deep Cryogenic Treatment of Metallic Materials in Automotive Applications. Metals, 10(4): 434.

Kaseem, M., Kamil, M.P., Kwon, J.H., Ko, Y.G., 2015, Effect of sodium benzoate on corrosion behavior of 6061 Al alloy processed by plasma electrolytic oxidation. Surface and Coatings Technology, 283: 268-273, doi:https://doi.org/10.1016/j.surfcoat.2015.11.006.

Ko, D.-H., Ko, D.-C., Lim, H.-J., Lee, J.-M., Kim, B.-M., 2013, Prediction and measurement of relieved residual stress by the cryogenic heat treatment for Al6061 alloy: Mechanical properties and microstructure. Journal of Mechanical Science and Technology, 27, doi:10.1007/s12206-013-0601-1.

Lam, D., Menzemer, C., Srivatsan, T., 2010, A study to evaluate and understand the response of aluminum alloy 2026 subjected to tensile deformation. Materials & Design, 31: 166-175, doi:10.1016/j.matdes.2009.06.040.

Lulay, K.E., Khan, K., Chaaya, D., 2002, The effect of cryogenic treatments on 7075 aluminum alloy. Journal of Materials Engineering and Performance, 11(5): 479-480, doi:10.1361/105994902770343683.

Ma, A., Saito, N., Shigematsu, I., Suzuki, K., Takagi, M., Nishida, Y., Iwata, H., Imura, T., 2004, Effect of Heat Treatment on Impact Toughness of Aluminum Silicon Eutectic Alloy Processed by Rotary-Die Equal-Channel Angular Pressing. Materials Transactions - MATER TRANS, 45: 399-402, doi:10.2320/matertrans.45.399.

REFERENCES (continued)

Macário, P.F., Vieira, A., Manfroi, L., da Silva, M.G.P., Leite, P., Vieira, L., 2019, Corrosion behavior of Al2024-T3, Al5052-H32, and Al6061-T6 aluminum alloys coated with DLC films in aviation fuel medium, Jet A-1 and AVGAS 100LL. Materials and Corrosion, 70(12): 2278-2291, doi:10.1002/maco.201911035.

Maisonnette, D., Suery, M., Nelias, D., Chaudet, P., Epicier, T., 2011, Effects of heat treatments on the microstructure and mechanical properties of a 6061 aluminium alloy. Materials Science and Engineering: A, 528(6): 2718-2724, doi:https://doi.org/10.1016/j.msea.2010.12.011.

Marioara, C.D., Nordmark, H., Andersen, S.J., Holmestad, R., 2006, Post-β″ phases and their influence on microstructure and hardness in 6xxx Al-Mg-Si alloys. Journal of Materials Science, 41(2): 471-478, doi:10.1007/s10853-005-2470-1.

Mascagni, D.B.T., Souza, M.E.P.d., Freire, C.M.d.A., Silva, S.L., Rangel, R.d.C.C., Cruz, N.C.d., Rangel, E.C., 2014, Corrosion resistance of 2024 aluminum alloy coated with plasma deposited a-C:H:Si:O films. Materials Research, 17: 1449-1465.

Ozturk, F., Sisman, A., Toros, S., Kilic, S., Picu, R.C., 2010, Influence of aging treatment on mechanical properties of 6061 aluminum alloy. Materials & Design, 31(2): 972-975, doi:https://doi.org/10.1016/j.matdes.2009.08.017.

Padmini, B.V., Sampathkumaran, P., Seetharamu, S., Jaiprakash, N., Niranjan, H., 2019a, Investigation on the wear behaviour of Aluminium alloys at cryogenic temperature and subjected to cryo -treatment. IOP Conference Series: Materials Science and Engineering, 502: 012191, doi:10.1088/1757-899X/502/1/012191.

REFERENCES (continued)

Padmini, B.V., Sampathkumaran, P., Seetharamu, S., Naveen, G.J., Niranjan, H.B., 2019b, Investigation on the wear behaviour of Aluminium alloys at cryogenic temperature and subjected to cryo -treatment. IOP Conference Series: Materials Science and Engineering, 502: 012191, doi:10.1088/1757-899x/502/1/012191.

Pantelakis, S., Setsika, D., Chamos, A., Zervaki, A., 2016, Corrosion damage evolution of the aircraft aluminum alloy 2024 T3. International Journal of Structural Integrity, 7(1): 25-46, doi:10.1108/IJSI-03-2014-0010.

Pantelakis, S.G., Chamos, A.N., Kermanidis, A.T., 2012, A critical consideration for the use of Al-cladding for protecting aircraft aluminum alloy 2024 against corrosion. Theoretical and Applied Fracture Mechanics, 57(1): 36-42, doi:https://doi.org/10.1016/j.tafmec.2011.12.006.

Park, D.-H., Choi, S.-W., Kim, J.-H., Lee, J.-M., 2015, Cryogenic mechanical behavior of 5000- and 6000-series aluminum alloys: Issues on application to offshore plants. Cryogenics, 68: 44-58, doi:https://doi.org/10.1016/j.cryogenics.2015.02.001.

Reboul, M.C., Baroux, B., 2011, Metallurgical aspects of corrosion resistance of aluminium alloys. Materials and Corrosion, 62(3): 215-233, doi:https://doi.org/10.1002/maco.201005650.

Salguero, J., Del Sol, I., Gómez-Parra, Á., Batista Ponce, M., 2020, Machining of Al-Cu and Al-Zn Alloys for Aeronautical Components. 10.5772/intechopen.93719

Shi, H., Han, E.-H., Liu, F., Kallip, S., 2013, Protection of 2024-T3 aluminium alloy by corrosion resistant phytic acid conversion coating. Applied Surface Science, 280: 325-331, doi:https://doi.org/10.1016/j.apsusc.2013.04.156.

REFERENCES (continued)

Siskou, N., Charalampidou, C., Alexopoulos, N.D., Kourkoulis, S.K., 2018, Effect of corrosion exposure on aluminum alloy 2024 for different artificial ageing conditions. Procedia Structural Integrity, 10: 79-84, doi:https://doi.org/10.1016/j.prostr.2018.09.012.

Snihirova, D., Höche, D., Lamaka, S., Mir, Z., Hack, T., Zheludkevich, M.L., 2019, Galvanic corrosion of Ti6Al4V -AA2024 joints in aircraft environment: Modelling and experimental validation. Corrosion Science, 157: 70-78, doi:https://doi.org/10.1016/j.corsci.2019.04.036.

Valerie, G., Georges, M., 1999, Localized corrosion of 2024 T352 aluminium alloy in chloride media. Corrosion Science 41: 421–438.

Varun Chandra, M., Sudarshan, M., Sumantha, H., Harshith Gowda, K.I., 2018, Effect of with and without cryogenic treatment on Tensile, hardness and impact on hybrid Aluminium-6061 metal matrix composites. International Journal of Engineering Research and General Science, 6(3).

Wang, J., Fu, R., Li, Y., Zhang, J., 2014, Effects of deep cryogenic treatment and low-temperature aging on the mechanical properties of friction-stir-welded joints of 2024-T351 aluminum alloy. Materials Science and Engineering: A, 609: 147–153, doi:10.1016/j.msea.2014.04.077.

Xiangfeng, M., Wei, G., Hongliang, G., Yundan, Y., Ying, C., Dettinger, H., 2013, Anodization for 2024 Al Alloy from Sulfuric-Citric Acid and Anticorrosion Performance of Anodization Films. International Journal of Electrochemical Science, 8: 10660-10671.

Zhang, W.D., Yang, J., Dang, J.Z., Liu, Y., Xu, H., 2013, Effects of Cryogenic Treatment on Mechanical Properties and Corrosion Resistance of LC4 Aluminum Alloy. Advanced Materials Research, 627: 694-697, doi:10.4028/www.scientific.net/AMR.627.694.

REFERENCES (continued)

Zheng, K., Politis, D.J., Wang, L., Lin, J., 2018, A review on forming techniques for manufacturing lightweight complex—shaped aluminium panel components. International Journal of Lightweight Materials and Manufacture, 1, doi:10.1016/j.ijlmm.2018.03.006.

Zhou, J., Xu, S., Huang, S., Meng, X.K., Sheng, J., Zhang, H., Li, J., Sun, Y., Agyenim-Boateng, E., 2016, Tensile Properties and Microstructures of a 2024-T351 Aluminum Alloy Subjected to Cryogenic Treatment. Metals, 6: 279, doi:10.3390/met6110279.